University of Windsor
Scholarship at UWindsor

Electronic Theses and Dissertations

2000

A time series analysis on the prospective relationships between the water level dynamics of Lake Erie and the El Nino/Southern Oscillation phenomenon.

Christopher Robert. Johnston
University of Windsor

Follow this and additional works at: http://scholar.uwindsor.ca/etd

Recommended Citation
Johnston, Christopher Robert., "A time series analysis on the prospective relationships between the water level dynamics of Lake Erie and the El Nino/Southern Oscillation phenomenon." (2000). *Electronic Theses and Dissertations.* Paper 855.

This online database contains the full-text of PhD dissertations and Masters' theses of University of Windsor students from 1954 forward. These documents are made available for personal study and research purposes only, in accordance with the Canadian Copyright Act and the Creative Commons license—CC BY-NC-ND (Attribution, Non-Commercial, No Derivative Works). Under this license, works must always be attributed to the copyright holder (original author), cannot be used for any commercial purposes, and may not be altered. Any other use would require the permission of the copyright holder. Students may inquire about withdrawing their dissertation and/or thesis from this database. For additional inquiries, please contact the repository administrator via email (scholarship@uwindsor.ca) or by telephone at 519-253-3000ext. 3208.

INFORMATION TO USERS

This manuscript has been reproduced from the microfilm master. UMI films the text directly from the original or copy submitted. Thus, some thesis and dissertation copies are in typewriter face, while others may be from any type of computer printer.

The quality of this reproduction is dependent upon the quality of the copy submitted. Broken or indistinct print, colored or poor quality illustrations and photographs, print bleedthrough, substandard margins, and improper alignment can adversely affect reproduction.

In the unlikely event that the author did not send UMI a complete manuscript and there are missing pages, these will be noted. Also, if unauthorized copyright material had to be removed, a note will indicate the deletion.

Oversize materials (e.g., maps, drawings, charts) are reproduced by sectioning the original, beginning at the upper left-hand corner and continuing from left to right in equal sections with small overlaps.

Photographs included in the original manuscript have been reproduced xerographically in this copy. Higher quality 6" x 9" black and white photographic prints are available for any photographs or illustrations appearing in this copy for an additional charge. Contact UMI directly to order.

Bell & Howell Information and Learning
300 North Zeeb Road, Ann Arbor, MI 48106-1346 USA
800-521-0600

A Time Series Analysis on the Prospective Relationships Between the Water Level Dynamics of Lake Erie and the El Niño/Southern Oscillation Phenomenon

by

Chris Johnston

A Thesis
Submitted to the College of Graduate Studies and Research
through the Department of Earth Sciences
in Partial Fulfillment of the Requirements for
the Degree of Master of Arts at the
University of Windsor

Windsor. Ontario, Canada

2000

© 2000 Chris Johnston

National Library of Canada
Acquisitions and Bibliographic Services
395 Wellington Street
Ottawa ON K1A 0N4
Canada

Bibliothèque nationale du Canada
Acquisitions et services bibliographiques
395, rue Wellington
Ottawa ON K1A 0N4
Canada

Your file Votre référence

Our file Notre référence

The author has granted a non-exclusive licence allowing the National Library of Canada to reproduce, loan, distribute or sell copies of this thesis in microform, paper or electronic formats.

L'auteur a accordé une licence non exclusive permettant à la Bibliothèque nationale du Canada de reproduire, prêter, distribuer ou vendre des copies de cette thèse sous la forme de microfiche/film, de reproduction sur papier ou sur format électronique.

The author retains ownership of the copyright in this thesis. Neither the thesis nor substantial extracts from it may be printed or otherwise reproduced without the author's permission.

L'auteur conserve la propriété du droit d'auteur qui protège cette thèse. Ni la thèse ni des extraits substantiels de celle-ci ne doivent être imprimés ou autrement reproduits sans son autorisation.

0-612-52582-1

Canada

ABSTRACT

In an attempt to gain a better understanding of Lake Erie water level dynamics, this study asseses the relationship between the Lake Erie water balance and the El Niño/Southern Oscillation (ENSO) phenomenon using data collected from 1950-1998. After standardizing the collected data, Box-Jenkins time series techniques were utilized assess the temporal patterns and interrelationships of the Multivariate ENSO Index and the Lake Erie water balance variables. The temporal patterns of Lake Erie water levels (LEWL), Lake Erie net basin supply (LENBS), and Lake Erie outflows (LERO) were best described by an AR (1) model. The Multivariate ENSO Index (MEI) was best described by an ARMA (1,0,1) (1,0,0) model, with a seasonal lag of 5. Lake St. Clair outflow (LSCO) was best fit to an ARMA (1,0,1) model. The time-ordered findings here complement the findings of others such as Guetter et al. (1995), LaValle et al. (1999), and Wang et al. (1999).

Significant relationships exist between the Lake Erie hydrologic variables tested and the Multivariate ENSO Index. With MEI lagged 3 1/2 years as an independent regressor against LEWL, LSCO, and LERO, weak, direct relationships were discovered. These relationships can be accepted under the condition that weak impacts of ENSO in the Lake Erie basin are to be expected. With MEI lagged 2 years as an independent regressor against LENBS, a weak inverse relationship exists. This relationship may be the result of an averaged time lag between the effects of ENSO on temperature/air pressure patterns (lag = 3 months) and precipitation (lag = 3 1/4 years) off the west coast of North America.

Because the MEI is a relatively new measure of the state of ENSO, little research has been completed using the MEI as an independent regressor variable. As such, the findings in this study merely represent a stepping stone to build from, and should not be considered as definitive. Future studies of the relationship between Great Lakes water levels and the ENSO phenomenon may be best served to incorporate both Southern Oscillation Index (SOI) and MEI, to determine any differences the two indices may have.

ACKNOWLEDGEMENTS

I would like to extend full gratitude to those people whose contributions helped make this research possible. I would like to thank Dr. Ana da Silva and Dr. V.C. Lakhan for their insight and help as members of my thesis committee. I would also like to thank my supervisor, Dr. P.D. La Valle, for his time and dedication to this research. Special thank yous are extended to Dr. Klaus Wolter - NOAA and David Faye - Environment Canada, for supplying the raw data used in this research. Without their contributions, this research could not have been made possible. A final thank you goes out to all of my family and friends - I wish you all a permanent smile.

TABLE OF CONTENTS

Chapter 1.0 Introduction 1

Chapter 2.0 The Study Area 3

Chapter 3.0 Literature Review 7

3.1 The Water Balance of Lake Erie 7

3.1.1 *Model # 1* 7

3.1.2 *Model # 2* 9

3.2 ENSO 10

3.2.1 Measuring the State of ENSO 11

3.2.2 A Historical Perspective of the Effects of ENSO 13

Chapter 4.0 Conceptual Approach 15

4.1 A Priori Model 15

4.2 Hypotheses 18

Chapter 5.0 Methodology 24

5.1 Data Collection 24

5.2 Methodology 24

5.3 The Box-Jenkins Approach vs. Spectral Analysis 26

Chapter 6.0 Results 28

6.1 Lake Erie Water Levels 44

6.2 The Multivariate ENSO Index 48

6.3 Lake Erie Net Basin Supply 50

6.4 Lake St. Clair Outflow 52

6.5 Lake Erie Outflow 52

6.6 Cross-Correlations 55

6.7 ARMA With Lagged Regressors Models of Lake Erie Hydrologic Parameters..... 60
6.7.1 The LEWL-MEI Model..... 60
6.7.2 The LENBS-MEI Model..... 62
6.7.3 The LSCO-MEI Model..... 62
6.7.4 The LERO-MEI Model..... 65
6.8 A Comparison Between MEI and SOI..... 67
Chapter 7.0 Discussion and Conclusions..... 68
7.1 Discussion..... 68
7.2 Conclusions..... 70
7.3 Limitations Associated with the Multivariate ENSO Index..... 71
References..... 72
Appendix: General Circulation of the Atmosphere..... 76
Vita Auctoris..... 78

LIST OF TABLES

Table 1: ARMA REGRESSION MODEL OF B.C. TEMPERATURE AND SOI..... 20

Table 2: ARMA REGRESSION MODEL OF B.C. RAINFALL AND SOI..... 20

Table 3: LEWL TEMPORAL MODEL FIT (1, 0, 0)..... 44

Table 4: LEWL TEMPORAL MODEL FIT (2, 0, 0)..... 45

Table 5: MEI TEMPORAL MODEL FIT..... 48

Table 6: LENBS TEMPORAL MODEL FIT..... 50

Table 7: LSCO TEMPORAL MODEL FIT..... 52

Table 8: LERO TEMPORAL MODEL FIT..... 55

Table 9: MODEL OF LAKE ERIE WATER LEVELS AND MEI..... 62

Table 10: MODEL OF LAKE ERIE NET BASIN SUPPLY AND MEI..... 62

Table 11: MODEL OF LAKE ST. CLAIR OUTFLOWS AND MEI..... 65

Table 12: MODEL OF LAKE ERIE OUTFLOWS AND MEI..... 67

Table 13: MULTIPLE REGRESSION RESULTS OF MEI AND SOI..... 67

LIST OF FIGURES

Figure 1: The Great Lakes Basin..... 5

Figure 2: Bathymetry of Lake Erie and Lake St. Clair..... 6

Figure 3: A priori model.....17

Figure 4: Autocorrelation Function - B.C. Temperature/SOI Residuals From An AR (1) Model. Independent Regressor: SOI - 3 Month Lag..... 21

Figure 5: Autocorrelation Function - B.C. Rainfall/SOI Residuals From An AR (1) Model. Independent Regressor: SOI - 3.25 Year Lag... 22

Figure 6: A Time Series Plot of Standardized Lake Erie Water Levels..... 29

Figure 7: A Time Series Plot of the Multivariate ENSO Index.....30

Figure 8: A Time Series Plot of Standardized Lake Erie Net Basin Supply.. 31

Figure 9: A Time Series Plot of Standardized Lake St. Clair Outflow..... 32

Figure 10: A Time Series Plot of Standardized Lake Erie Outflow..... 33

Figure 11: Autocorrelation Function - Standardized Lake Erie Water Levels..... 34

Figure 12: Partial Autocorrelation Function - Standardized Lake Erie Water Levels.....35

Figure 13: Autocorrelation Function - Standardized Quarterly Multivariate ENSO Index (MEI) Values..... 36

Figure 14: Partial Autocorrelation Function - Standardized Quarterly Multivariate ENSO Index (MEI) Values..... 37

Figure 15: Autocorrelation Function - Standardized Lake Erie Net Basin Supply..... 38

Figure 16: Partial Autocorrelation Function - Standardized Lake Erie Net Basin Supply..... 39

Figure 17: Autocorrelation Function - Standardized Lake St. Clair Outflow..... 40

Figure 18: Partial Autocorrelation Function - Standardized Lake St. Clair Outflow..... 41

Figure 19: Autocorrelation Function - Standardized Lake Erie Outflow... 42

Figure 20: Partial Autocorrelation Function - Standardized Lake Erie Outflow..... 43

Figure 21: Autocorrelation Function - Lake Erie Water Level Residuals From An AR (1) Model. Intervention Analysis at Case Number 92..... 46

Figure 22: Autocorrelation Function - Lake Erie Water Level Residuals From An AR (2) Model. Intervention Analysis at Case Number 92..... 47

Figure 23: Autocorrelation Function - Quarterly Multivariate ENSO Index Residuals From An ARMA (1, 0, 1) (1, 0, 0) Model. Intervention Analysis at Case Number 92; Seasonal Lag of 5..... 49

Figure 24: Autocorrelation Function - Lake Erie Net Basin Supply Residuals From An AR (1) Model..... 51

Figure 25: Autocorrelation Function - Lake St. Clair Outflow Residuals From An ARMA (1, 0, 1) Model. Intervention Analysis at Case Number 92..... 53

Figure 26: Autocorrelation Function - Lake Erie Outflow Residuals From An AR (1) Model. Intervention Analysis at Case Number 92..... 54

Figure 27: Cross-Correlation Function - Standardized Lake Erie Water Levels; Lagged: Quarterly Multivariate ENSO Index Values..... 56

Figure 28: Cross-Correlation Function - Standardized Lake Erie Net Basin Supply; Lagged: Quarterly Multivariate ENSO Index Values..... 57

Figure 29: Cross-Correlation Function - Standardized Lake St. Clair Outflow; Lagged: Quarterly Multivariate ENSO Index Values..... 58

Figure 30: Cross-Correlation Function - Standardized Lake Erie Outflow; Lagged: Quarterly Multivariate ENSO Index Values..... 59

Figure 31: Autocorrelation Function - LEWL/MEI Residuals From An AR (1) Model. Independent Regressor: MEI - 3 1/2 Year Lag..... 61

Figure 32: Autocorrelation Function - LENBS/MEI Residuals From An AR (1) Model. Independent Regressor: MEI - 2 Year Lag..... 63

Figure 33: Autocorrelation Function - LSCO/MEI Residuals From An ARMA (1, 0, 1) Model. Independent Regressor: MEI - 3 1/2 Year Lag..... 64

Figure 34: **Autocorrelation Function - LERO/MEI Residuals From An AR (1) Model. Independent Regressor: MEI - 3 1/2 Year Lag..... 66**

1.0 Introduction

Lake Erie, the fourth largest of the Great Lakes, is a major water resource shared by the United States and Canada. The lake contains 484 km^3 of water with 25,700 km^2 of surface area and 78,000 km^2 of land drainage area in the basin (which includes the Lake St. Clair/Detroit River system; NOAA, 1999). Along with its connecting channels, the Detroit and Niagara rivers, Lake Erie is intensively used for recreation and navigation. The surrounding shorelines of Lake Erie are highly developed, but are exposed to both natural and human phenomena that can lead to detrimental changes within the area's system. Changes in water levels are also a result of natural and human phenomena and, while a number of explanations have been offered as to why Lake Erie water levels continue to fluctuate over time, there still needs to be further research conducted in order to fully understand these variations.

Explanations that have been proposed to account for the fluctuations in Lake Erie water levels include the effects of precipitation, evaporation, runoff, water inflows and outflows, and the consumptive use of water (Quinn, 1978; Bruce, 1984; Quinn and Guerra, 1986). Lake Erie water levels, and its influencing components (net basin supply, Detroit River inflow, Niagara River outflow, Welland Diversion outflow) in particular, may also be fluctuating in response to El Niño/Southern Oscillation (ENSO) events. In this study, there is an attempt to rationalize this premise under a statistical analysis approach.

This research is based on the rationale that ENSO may have forcing mechanisms upon the atmospheric systems that govern evaporation and precipitation patterns that influence lake level dynamics. Previous research (Halpert et al., 1993; Bell and Janowiak, 1995; Guetter and Georgakakos, 1996; LaValle et al., 1999) has shown a connection between ENSO events and regional water body dynamics. However, there has been no previous attempt to monitor the long-term changes in Lake Erie water level dynamics, as related to the ENSO phenomenon. This relatively unique study explores the possibility of existing relationships between ENSO events and several water balance components of Lake Erie, in an attempt to gain a better understanding

of the lake's water level dynamics. It is imperative that hydrologists and shoreline engineers have a vast comprehension of water level dynamics before proceeding with any water management or shoreline protection strategies.

2.0 The Study Area

Lake Erie forms the boundary between Canada (Ontario) to the north and the United States (Michigan, Ohio, Pennsylvania, and New York) to the west, south, and east (see Figure 1). The major axis of the lake extends from west-southwest to east-northeast for 388 km, and the maximum width of the lake is 92 km. The lake's principal tributary rivers are the Detroit (which carries the discharge of Lake Huron), Huron, and Raisin rivers of Michigan; the Maumee, Portage, Sandusky, Cuyahoga, and Grand rivers of Ohio; the Cattaraugus Creek of New York; and the Grand River of Ontario (britannica.com, 1999). The lake discharges at its eastern end through the Niagara River and the Welland Diversion.

Lake Erie is the shallowest of the Great Lakes, with a maximum depth of 210 ft (see Figure 2 for bathymetry of Lake Erie; depth measured in meters). Thus, the lake becomes highly vulnerable to fluctuating water levels. Wind setups (wind that pushes water from one end of the lake toward the other, usually onshore), primarily from west to east/north-east, have in the past produced large short-term differences in water levels at the eastern and western ends of the lake, with the record being more than 16 ft (Environment Canada and the U.S. Environmental Protection Agency, 1995). These short-term fluctuations (due to wind setups) can lead to temporary increases and decreases in Niagara River flows and to the stimulation of flow reversals in the lower Detroit River, which ultimately will lead to a disruption of the overall water balance of Lake Erie (great-lakes.net).

Annual or seasonal variations in the water levels of Lake Erie are based primarily on the changes in precipitation, runoff, and evaporation. Generally, the lowest levels occur in the winter when much of the precipitation is locked up in snow and ice, and dry winter air masses pass over the lake enhancing evaporation. Lake levels are highest in the summer after the spring thaw when runoff increases. While it is known that long-term variations in lake levels can be attributed to the changes in net basin supplies over time (Quinn and Guerra, 1986), the causes of these variations

have yet to be adequately explained. This research will attempt to link the ENSO phenomenon with the long-term water balance changes of Lake Erie.

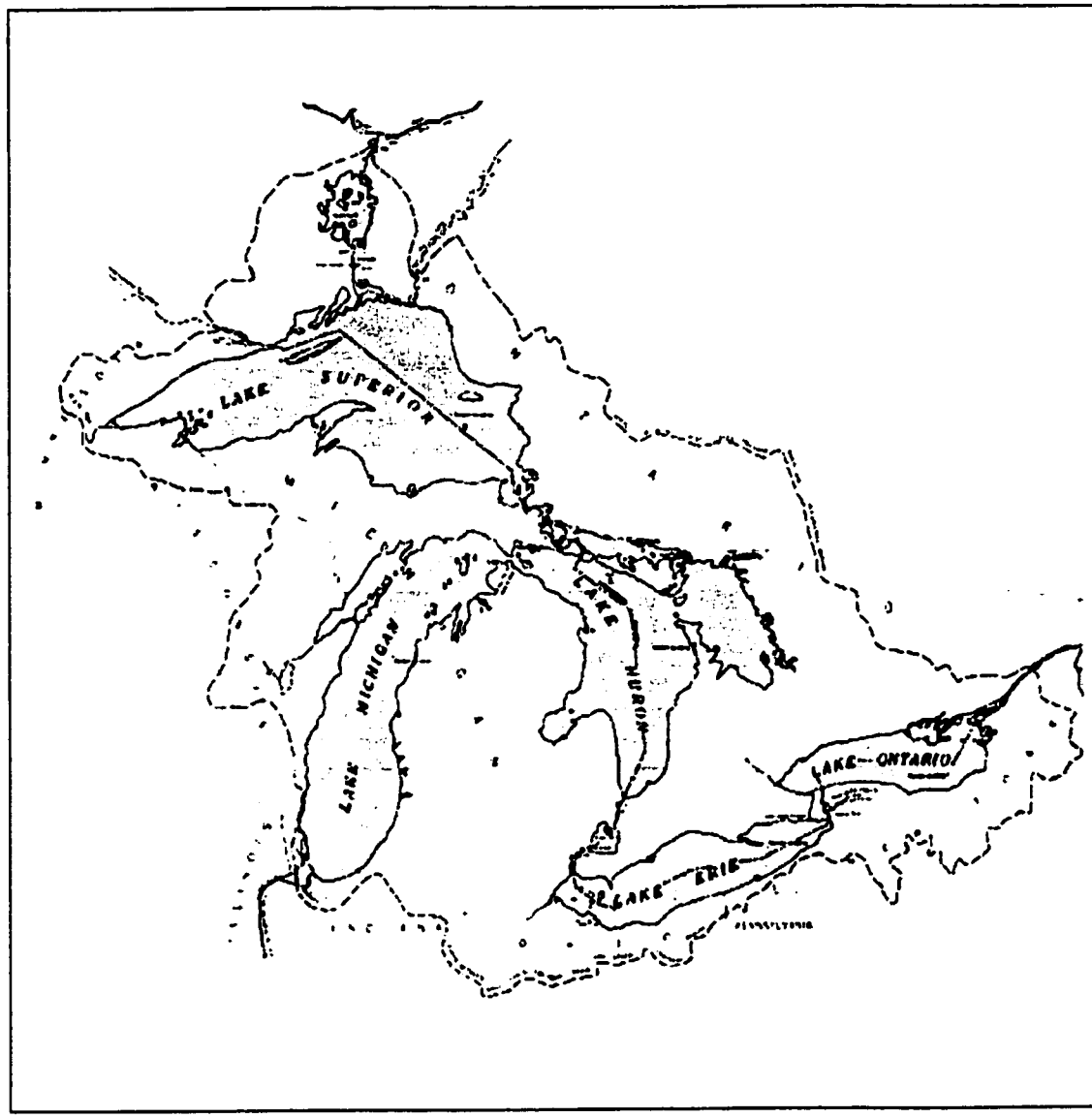

Figure 1. The Great Lakes Basin.
Taken directly from the website:
chswww.bur.dfo.ca/danp/images/fig3.gif

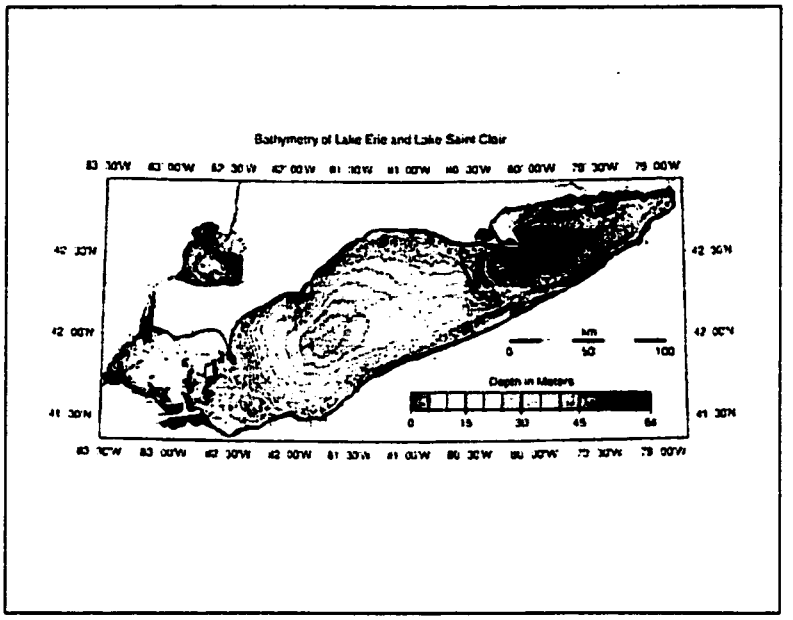

Figure 2. Bathymetry of Lake Erie and Lake St. Clair.
Taken directly from the website:
www.ngdc.noaa.gov/mgg/greatlakes/lakeerie_cdrom/images/le.jpg

3.0 Literature Review

Within the Great Lakes (Lake Erie in particular), the latter half of the twentieth century has produced record high water levels in the years 1974 and 1986 (Meadows et al., 1997). However, over the last twenty years (including 1988 and 1995), severe decreases in Lake Erie water levels have also been observed (LaValle and Lakhan, 1997; LaValle et al., 1999). In essence, water levels in Lake Erie have shown significant fluctuations over the past half-century. These significant fluctuations may be a result of the El Niño/Southern Oscillation (ENSO) phenomenon. The proceeding literature details the evolution and theory behind 1) Lake Erie's water balance and 2) ENSO.

3.1 The Water Balance of Lake Erie

In recent decades, studies of Lake Erie water balance components have been undertaken by Brunk (1964), Sanderson (1966), Jones and Meredith (1972), and Derecki (1976). In the majority of these studies, there was an emphasis on determining the various components of the water balance without regard to the mass continuity of the system. Quinn (1978) has previously proposed that system continuity is an important consideration in studies of Great Lakes response models. Consequently, the majority of these studies have failed to properly assess the continuity of the Lake Erie water balance. The following two models offer system continuity equations to solve the Lake Erie water balance over a given time period.

3.1.1 *Model # 1*

Quinn and Guerra (1986) examined the Lake Erie water balance based on the individual components for 1940-79, with a particular emphasis on the continuity of the system. In their study, system continuity was analyzed on both an annual and monthly basis. The continuity equation for Lake Erie was expressed as:

$$Q_n + D + CU +/- S - S_t - Q_d - P - R + E = r \qquad (1)$$

where Q_n is the outflow through the Niagara River, D is the outflow through the Welland Diversion, CU is the consumptive use of water from the lake, S is the change in lake storage as

measured by the water level gauges, S_t is the change in lake storage due to thermal expansion, Q_d is the inflow from the Detroit River, P is the precipitation falling on the lake surface, R is the runoff from the lake drainage basin, E is the evaporation from the lake surface, and r is a residual (if continuity is satisfied; then r = 0).

The total water supply to Lake Erie comes from a combination of the Detroit River flow and the net basin supply (NBS) defined as:

$$NBS = P + R - E \qquad (2)$$

Quinn and Guerra (1986) have inferred that approximately 87% of the total water supply to Lake Erie is provided by the Detroit River, while only 13% is provided by the net basin supply. However, this comparison was found to be misleading, as it is not the relative magnitudes of the supply components (but their relative variabilities) that determine their respective impacts on lake level variations. Although the magnitude of the Detroit River is about seven times the magnitude of the annual net basin supply, its variability is only twice as large. Subsequently, this results in the net basin supply being a significant factor in the simulation, hindcasting, and forecasting of Lake Erie water levels.

In various regulation and management studies (e.g. IGLLB, 1973), the net basin supply has been computed as a residual from equation (1) rather than independently as in equation (2). According to Quinn and Guerra (1986), the net basin supply can be computed by setting the residual r equal to zero and arranging equation (1) as:

$$NBS = Q_n + D + CU + S - S_t - Q_d \qquad (3)$$

The significance of the differences between the two procedures is that, when evaluating management alternatives, it is necessary to evaluate past water supplies under current channel conditions. By using equation (3), the computations would be bias from incorporating errors in connecting channel flow measurements due to measurement techniques or the computation of regime changes.

3.1.2 *Model # 2*

Lee et al. (1998) developed a hydrologic response model of the unregulated Great Lakes - Lakes Erie, St.Clair, and Michigan-Huron. The model consists of water balances and channel routing dynamics combined to estimate lake levels and connecting channel flows from water to the lakes. The following mass continuity equation (an advancement over Quinn and Guerra's), expressed for each lake in terms of quarter-monthly rates of inflow, outflow, and change in lake storage, is solved for the change in each lake's water level over a time interval:

$$P + R + Q_u - QR_u \pm D \pm G = E + C + Q_d - QR_d + A(\Delta Z/\Delta t) \qquad (1)$$

where inflows are precipitation over the lake's surface (P), watershed runoff (R), diversions to the lake or its watershed (+D), groundwater contributions (+G), and inflows via the upstream connecting channel (Q_u) minus flow retardation due to ice or weed growth (QR_u). Outflows are evaporation from the lake surface (E), consumptive uses (C), diversion from the lake or its watershed (-D), groundwater losses (-G), and outflows via its downstream connecting channel (Q_d) minus flow retardation due to its ice or weed growth (QR_d). The change in lake storage is estimated by multiplying the lake area (A) by the change in lake elevation ($\Delta Z = Z^t - Z^{t-1}$) over a time interval (Δt).

The connecting channel inflow and outflow rates over the time interval are approximated by the equation:

$$Q = Q_t + 1/2(\delta Q_t/\delta t)\Delta t \qquad (2)$$

The connecting channel flows are computed using stage-discharge equations of the basic form (derived from Manning's flow equation):

$$Q^t = K[\varphi Z_u^t + (1 - \varphi)Z_d^t - ym]^a (Z_u^t - Z_d^t)^b \qquad (3)$$

where Q^t is the lake outflow and Z^t is lake level at the beginning of the time interval. The subscripts u and d denote the lakes upstream and downstream of the connecting channel, respectively. Constants in the equation are K, a coefficient related to channel cross-section characteristics (roughness, hydraulic radius, and area), φ (ranging between .5 and 1), a and b

(theoretically 5/3 and 1/2, respectively), and ym, which represents the mean bottom elevation of the connecting channel.

3.2 ENSO

The tropical Pacific encompasses a large zonal contrast in sea surface temperature (SST) along the equator, with a warm pool in the west and a cold tongue in the east. Within this cold tongue are strong SST interannual fluctuations (Jin, 1998). The El Niño/Southern Oscillation phenomenon (ENSO), which affects much of the global climate, is a dominant factor to the interannual variability within the cold tongue region. There has been great progress made over the past decade to understanding and predicting ENSO (refer to Jin (1998) for a complete list of references).

Bjerknes (1969) was the first to hypothesize that a positive feedback of tropical ocean-atmosphere interaction can amplify SST perturbations of the cold tongue to sustain either a warm (El Niño) or cold phase (La Niña) of ENSO. The easterly trade winds force the thermocline depth to be shallower in the equatorial eastern Pacific than in the western Pacific, and they induce the equatorial Ekman upwelling, which effectively brings cold water to the surface layer to generate a cold tongue in the eastern Pacific. The Walker circulation (an equatorial zonal asymmetric circulation), is driven by the atmospheric zonal pressure gradient caused by the east-west contrast of the SST, which enhances the surface easterlies over the Pacific basin and thus strengthens the cold tongue. However, ultimately Bjerknes failed to uncover the phase transition mechanism for ENSO. Nearly two decades later it was found that during warm (cold) ENSO phases, the equatorial heat content is often draining out (building up) as a result of the mass exchange between the equatorial belt and off-equatorial regions through dynamical adjustment (Cane and Zebiak, 1985; Wyrtki, 1985; Cane al., 1986). These authors have proposed that a given discharge or recharge of the equatorial heat content is responsible for ENSO phase transitions. Jin (1997) has showed that this recharge-oscillation mechanism is at the heart of ENSO theory pointing to the instability of the tropical Pacific climate state, which further supports a delayed oscillator (Schopf

and Suarez. 1988; Battisti and Hurst, 1989) or a mixed SST-ocean dynamics mode (Jin and Neelin. 1993).

Jin (1998) has constructed a conceptual model describing the basic coupled dynamics of the tropical ocean atmosphere interaction. This model incorporates the positive feedback processes, which are responsible for the formation of the Pacific cold tongue and the growth of a warm or cold phase of ENSO, and memory residing in the ocean dynamic adjustment that is essential for the phase transition of the ENSO. Basically, when the cold tongue climate state is unstable (embraced by two super-critical Hopf bifurcations; refer to Jin (1998) for further explanation), an ENSO formation will result, which can be understood as an equatorial ocean recharge oscillator.

ENSO has been reasoned by Wang et al. (1999; refer to this paper for a more in-detail discussion of the following summary) of being stochastic in response. Although there are different mechanisms that may be at work in various phases of the ENSO evolutions (i.e. monsoons), they have been reasoned to be stochastic in nature. A produced model showed that an irregular ENSO-like oscillation arises from three different origins: stochastic resonance, coupled (i.e. atmospheric-ocean) non-linear instability, and stochastic transition. If the basic state happens to be stable, the stochastic forcing (defined as high frequency, unresolved physical processes) excites irregular oscillations by stochastic resonance. When the system is an unstable state, in which the coupled dynamics sustains a non-linear oscillation (stable limit cycle), the stochastic forcing disrupts the deterministic trajectory of the limit cycle in the phase space, generating irregularities and modifying the oscillation period. Finally, when the system possesses multi-equilibrium states, the stochastic forcing may produce an oscillatory system by randomly switching the system between a warm and cold stable steady state.

3.2.1 Measuring the State of ENSO

There are two known measurements of the state of ENSO: 1) the Southern Oscillation Index (SOI) and 2) the Multivariate ENSO Index (MEI). Previous research (for example:

Trenberth. 1990; Guetter and Georgakakos, 1996; Shabbar and Khandekar, 1996; Shabbar et al., 1997; LaValle et al., 1999) has correlated the SOI with atmospheric and hydrologic change in the northern hemisphere. In particular, the study of Shabbar et al. (1997) shows that the Great Lakes region is effected by the Southern Oscillation (SO) phenomenon when using the SOI as a measure of correlation between atmospheric and hydrologic patterns. During the first winter following the onset of El Niño (La Niña) events, a distinct pattern of negative (positive) precipitation anomalies were found to exist. Drier than normal conditions were shown to exist in the Lake Superior region during winter (+1) after an El Niño event. After a La Niña event, during the following winter the entire Great Lakes region was shown to have wetter than normal conditions. All of the significant precipitation anomolies were found to be explainable by the associated upper-atmospheric flow patterns, which during the first winter following the onset of El Niño (La Niña) events resemble the positive (negative) phase of the Pacific-North American pattern.

The Southern Oscillation is calculated as follows from the monthly (or seasonal) fluctuations in the sea level pressure difference between Tahiti and Darwin, Australia:

$$SOI = 10 (Pdiff - Pdiffav) / SD (Pdiff)$$

where Pdiff equals the average Tahiti mean sea level pressure (MSLP) for the month minus the average Darwin mean sea level pressure for the month. Pdiffav equals the long term average of Pdiff for the month in question, and SD (Pdiff) equals the standard deviation of Pdiff for the month in question (Australian Bureau of Meterology website). Sustained negative values of the SOI often indicate El Niño episodes. Negative values are often accompanied by sustained warming of the central and eastern tropical Pacific Ocean, and a decrease in the strength of the Pacific trade winds. Positive values of the SOI are associated with stronger Pacific trade winds and are often an indication of a La Niña episode.

The Multivariate ENSO Index is a relatively new measure of the state of ENSO, and as such little research has been completed using this variable. This study will be one of the first studies to attempt to correlate the MEI with regional hydrologic change. The MEI has been chosen

for this research because it provides more components and information than the SOI, and as such it should be a more sensitive variable (note - consult Chapter 6.8 for a comparitive analysis between SOI and MEI).

The Multivariate ENSO Index (MEI) bases itself on six main observed variables over the tropical Pacific (Wolter/NOAA, 1999). The six variables are: sea-level pressure (P), zonal (U) and meridional (V) components of the surface wind, sea surface temperature (S), surface air temperature (A), and total cloudiness fraction of the sky (C).

After spatially filtering the individual fields (located within the tropical Pacific) into clusters through cluster analysis (Wolter, 1987), the MEI is calculated as the first unrotated Principle Component (PC) of all six observed fields combined. According to Wolter and Timlin (1993), this is accomplished by normalizing the total variance of each field first, and then performing the extraction of the first PC on the co-variance matrix of the combined fields. The MEI is computed separately for each of twelve sliding bi-monthly seasons (Dec/Jan, Jan/Feb..... Nov/Dec).

To keep the MEI comparable, all seasonal values are standardized with respect to each season and to the given reference period. Positive values of the MEI represent the warm phase (El Niño) of ENSO, while negative values represent the cold phase (La Niña) of ENSO.

3.2.2 A Historical Perspective of the Effects of ENSO

From a historical perspective (in terms of the historical record) it is known that ENSO events can and will vary considerably in period and amplitude, thus having different climatic impacts on both a spatial and temporal basis (Quinn and Neal, 1992). With El Niño events, it is expected that there will be higher than normal winter temperatures and precipitation in those mid-latitude locations controlled by westerly wind systems (Philander, 1990). Sanderson (1993) has predicted that with climate change and higher temperatures, annual loss of water to the atmosphere through evapo-transpiration would have an increasing effect (on a given water supply), resulting in a decline in water flows and an increase in water deficiency. Since previous research (for example:

Ropelewski and Halpert, 1986, 1987, 1989; Kiladis and Diaz, 1989; Waylen et al., 1993; Shabbar and Khandekar, 1996; Stone et al., 1996; Kane, 1997; Shabbar et al., 1997) has shown that ENSO strongly influences regional and global variations in temperature and precipitation patterns, this research will attempt to show that ENSO events can influence the water level dynamics of Lake Erie.

4.0 Conceptual Approach

4.1 A Priori Model

A review of the literature has shown that ENSO events can have influencing effects on regional and global precipitation patterns. If precipitation can be affected by an El Niño or La Niña event. then it becomes reasonable to assume that the other two variables of net basin supply (runoff and evaporation) could also be subjected to significant changes when ENSO events are present within the Lake Erie system. Since net basin supply is directly related to total water supply. the water level dynamics of Lake Erie, in theory, should also alter under the presence of an ENSO event.

Lake Erie water levels have been depicted by LaValle et al. (1999) as being stochastic in nature. in terms of having an associated first order autoregressive process (AR 1). An AR (1) model describes what happens when a random shock is applied to a time series. with the effects persisting for several time intervals after the application of the shock (i.e. a 'long memory' response). In essence. the lake levels will have declining autocorrelation levels as the lag intervals increase. Kite (1992) ran a time series analysis on the monthly lake levels of Lake Erie at Cleveland. Ohio. and found that a second-order autoregressive component fit into his final model. A second-order autoregressive process. in a simplified definition. depicts a decaying pattern of autocorrelation levels. and becomes present where the output of a system is a response of what occurred at lag 2. Second-order processes are called Yule-Walker processes and they can be described by the equation:

$$z_t = \phi_1 z_{t-1} + \phi_2 z_{t-2} + a_t$$

where ϕ is the autoregressive parameter which describes the effect of a unit change in $z_{t+/-1, 2}$ on z_t. and a_t represents the random shock applied during the series (Vandaele, 1983).

Since net basin supply accounts for approximately 13% of the total Lake Erie water supply. it is within reason to predict that an autoregressive process will be concurrent with a net basin supply time series of Lake Erie. It is also reasonable to presume that the primary flows of

water. into and out of Lake Erie, will assume an autoregressive process (following Quinn and Guerra's (1986) water balance research). Based on these assumptions and the previous literature documented. an a priori model has been conceptualized (see Figure 3), in which the theoretical framework of the Lake Erie water balance is illustrated.

Figure 3, in part, is based on the previous work of Quinn and Guerra (1986; due to time and data constraints. Lee et al's (1998) hydrologic response model is not directly incorporated into this a priori model). This model is a re-creation of their system continuity equation for Lake Erie, with ENSO being an added component. Essentially, this model serves to detail the various interacting processes that comprise the Lake Erie water balance. Within this a priori model, to attain quarterly Lake Erie water levels, several stochastic processes will occur over time (consumptive use of water is not a randomly generated process: for the purposes of this investigation it will be ignored). Since the literature review (see Wang, 1999) has revealed that ENSO may be stochastic in nature, this model predicts the same will hold true for the net basin supply components (this is based on the rationale that ENSO events act as a feedback mechanism to the variables of net basin supply). Note - the changes in lake storage will not be evaluated against ENSO in this research, as the change in water levels should provide an adequate reflection of storage change.

In this model. the El Niño/Southern Oscillation phenomenon acts as a triggering mechanism on the Great Lakes climate system. Storm tracks, which originate from the Pacific Ocean and further develop off the west coast of North America (in particular. the province of British Columbia and the state of Washington), are altered during either an El Niño or La Niña event. which creates abnormal weather patterns, including the rise and fall in temperature in comparison to average seasonal conditions. These storm tracks subsequently head east (due to the presence of the prevailing westerlies in the northern hemisphere) and, after a lagged time period, the Great Lakes region will experience a significant change in lake strorage, due to the effects the storms have on the basin supplies (precipitation, runoff, evaporation. groundwater) within the

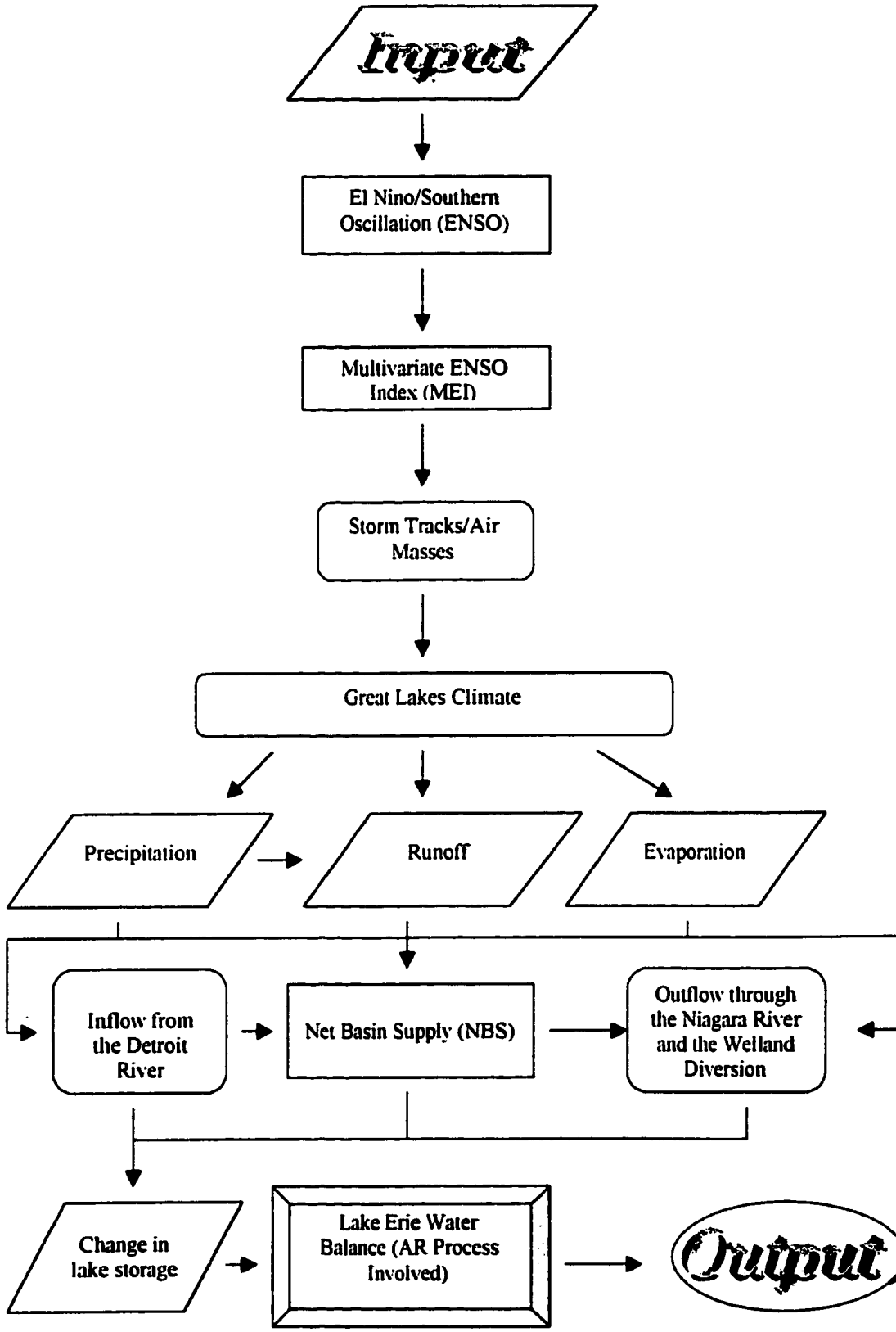

Figure 3. A priori model.

Source: Author, 2000.

region. As a result, an overall adjustment in the water balance of the lake will occur. For example, during periods of high precipitation, with low temperatures that reduce the evaporation process, discharge inflow from the Detroit River will be higher than normal. Under this scenario, an increase in the total water supply to the lake would occur. Providing one more example, during periods of warmer temperatures with decreased precipitation and runoff coupled with higher lake evaporation, lower net basin supplies result, which leads to a decrease in lake levels (over a lagged time period).

4.2 Hypotheses

The developed a priori model has conceptualized an interrelation between net basin supply, water flows, ENSO, and the overall water balance of Lake Erie. As a result, the following hypotheses are advanced:

1. Based on the previous research findings of Kite (1992), the LEWL model could be described by a 2nd order (psuedo-cyclic) Yule-Walker autoregressive process, which takes the form: $Y_t = \phi_{t-1} Y_{t-1} + \phi_{t-2} Y_{t-2} \pm \epsilon$; where ϵ is the error term and ϕ_i is the ith order autoregressive parameter estimate. However, Kite's analysis is based on monthly data and the second order autoregressive term may drop out with quarterly data due to aggregation effects.
2. Alternatively, the LEWL model may contain a 1st order autoregressive process, based on the semester data findings of LaValle et al. (1999). Since this study is based on quarterly data, a first-order autoregressive process is the more likely serial descriptor of Lake Erie water levels.
3. Lake Erie net basin supply (LENBS) should be fitted to a weak, first-order autoregressive process, based on Quinn and Guerra's (1986) assessment between net basin supply and the Lake Erie water balance. Weakened ENSO effects in the Lake Erie basin should be expected, due to the basin's distance away from the west coast of North America - where the effects of ENSO events can significantly influence cyclonic storm track patterns.
4. Since the outflows from Lake St. Clair (LSCO) are heavily influenced by outflows from Lakes Superior, Michigan, and Huron, one would expect a stronger serial process to be

operating on this variable, such as an AR (2) - Yule-Walker process or, an ARMA (1,0,1) autoregressive moving average process, which describes a pseudo-cyclic process with a shorter time period than an AR (2) model.

5. The Niagara River and Welland Diversion outflow (LERO) data should exhibit the same type of behaviour as the LEWL data, since outflow rates are directly controlled by Lake Erie water levels. Therefore, the serial behaviour of LERO should be described by either an AR (1) model, or an AR (2) model - which is the less probable model of the two.
6. Based on the findings of LaValle (2000), the serial behaviour of MEI seems to conform to a Yule Walker AR (2) process describing a pseudo-cyclic process. However, with quarterly data having a period of three months which is less than the four to five months period associated with a minimum length ENSO event, one might anticipate that an ARMA (1,0,1) (1,0,0) model could emerge, instead of the simple AR (2) model derived from semester data. Since major ENSO events tend to emerge in the month of May, a seasonal lag of 5 may describe the seasonal autoregressive term.
7. Lake Erie water level fluctuations (LEWL) should have a lagged relationship with the Multivariate ENSO Index (MEI), with the lag interval representing anywhere from 2-4 years (lags 8-16), since the average period beween ENSO events ranges from 2-4 years. Such a relationship should be tested in an ARIMA model with independent regressors (SPSS, 1999) which takes the form: $Y_t = \phi_1 Y_{t-1} + (\phi_2 Y_{t-2}$ - if needed) $+ \beta M_{t-k} \pm \epsilon$: where ϵ is the error term, β is the lagged regression coefficient, and ϕ_i is ith order autoregessive coefficent.
8. An ARIMA analysis of B.C. temperature and the Southern Oscillation Index has revealed that a significant relationship exists at lag 1 (3 months; see Table 1). SOI, with a lag of three months, was found to have an inverse relationship on B.C. temperature patterns ($r = -.327$) at a 95% level of significance. No significant autocorrelations were observed in the residuals of the independent regressor (SOI - lag 1) regression model (see Figure 4). An ARIMA analysis of B.C. rainfall and SOI has revealed that a significant inverse relationship exists at lag 13 (3

1/4 years; refer to Table 2). The independent regressor ARMA regression model (1, 0, 0) (1, 0, 0) explained 98.1% of the serial variation between the AR (1) and SOI (lag 13) components. The regression model residuals revealed that no significant autocorrelations were existing within the regressed variables (see Figure 5). These findings suggest that air pressure and temperature are affected on a much quicker basis than rainfall in the B.C. area, although the effects of ENSO persist in a similar manner (i.e. long memory, decaying effects) with the two climatic variables. Since temperature and air pressure can heavily influence evaporation rates, it is expected that the net basin supply of Lake Erie (factoring in the over-lake evaporation potential) will be affected by ENSO events approximately half-way between 3 months and 39 months. If such a relationship exists, it is expected to be quite weak, based on the logic outlined in hypothesis # 3. This could be tested in an ARIMA model with independent regressors, and the model would take the form: $Y_t = \phi_1 Y_{t-1} + (\phi_2 Y_{t-2}$ - if needed) $+ \beta M_{t-k} \pm \epsilon$; where ϵ is the error term, β is the lagged regression coefficient, and ϕ_i is ith order autoregessive coefficent.

TABLE 1. ARMA REGRESSION MODEL OF B.C. TEMPERATURE AND SOI
(Statistica '99 Output)

	B	SEB	T-RATIO	APPROX.	PROB.
AR1	.16203188	.07566018	2.1415741	.03364354
SOIL1	-.32717581	.08290074	-3.9465971	.00011558

$R^2 = .168$

TABLE 2. ARMA REGRESSION MODEL OF B.C. RAINFALL AND SOI
(Statistica '99 Output)

	B	SEB	T-RATIO	APPROX.	PROB.
AR1	.65787290	.06155464	10.687624	.0000000
SOIL13	-.19319359	.01676682	-11.522377	.0000000

$R^2 = .981$

Figure 4. Autocorrelation Function

B.C. Temperature/SOI Residuals From An AR (1) Model

Independent Regressor: SOI - 3 Month Lag

(Standard errors are white-noise estimates)

Lag	Corr.	S.E.	Q	p
1	+.004	.0752	.00	.9578
2	-.006	.0749	.01	.9951
3	-.023	.0747	.10	.9916
4	+.024	.0745	.21	.9950
5	+.059	.0743	.83	.9751
6	-.032	.0741	1.02	.9850
7	-.005	.0738	1.02	.9945
8	-.097	.0736	2.76	.9484
9	+.093	.0734	4.36	.8861
10	+.110	.0732	6.63	.7595
11	-.047	.0730	7.06	.7945
12	-.107	.0727	9.21	.6845
13	-.042	.0725	9.55	.7301
14	-.002	.0723	9.55	.7941
15	+.071	.0721	10.53	.7848

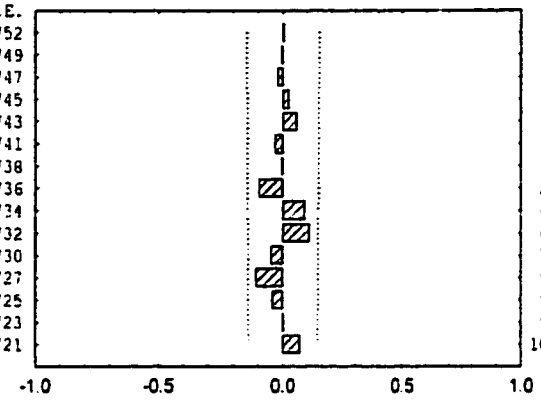

Corr. = Correlation; S.E. = Standard Error

Q = Box-Ljung Q statistic; p = probability value of the Q statistic

Figure 5. Autocorrelation Function

B.C. Rainfall/SOI Residuals From An AR (1) Model

Independent Regressor: SOI - 3.25 Year Lag

(Standard errors are white-noise estimates)

Lag	Corr.	S.E.	Q	p
1	-.062	.0752	.67	.4120
2	+.056	.0749	1.24	.5391
3	-.047	.0747	1.63	.6523
4	+.021	.0745	1.71	.7881
5	-.096	.0743	3.37	.6424
6	-.015	.0741	3.42	.7548
7	+.133	.0738	6.65	.4659
8	-.045	.0736	7.02	.5340
9	+.025	.0734	7.14	.6223
10	-.058	.0732	7.77	.6508
11	-.044	.0730	8.14	.7009
12	+.022	.0727	8.23	.7671
13	-.038	.0725	8.51	.8092
14	+.045	.0723	8.90	.9375
15	+.032	.0721	9.10	.8722

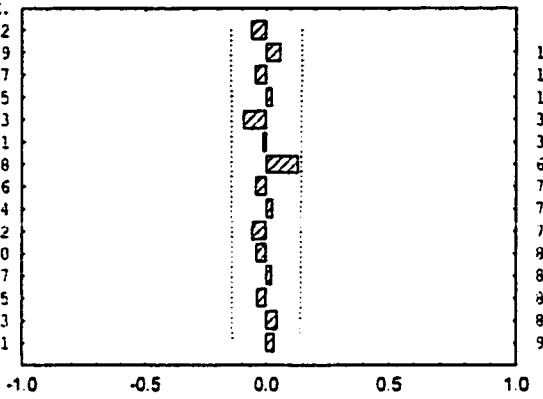

Corr. = Correlation; S.E. = Standard Error

Q = Box-Ljung Q statistic; p = probability value of the Q statistic

9. Since LSCO represents the inflow to Lake Erie from Lakes Huron, Michigan, and Lake Superior, one might expect that the influence of MEI could be stronger with respect to this variable, and it is hypothesized that such a relationship would take the form: $Y_t = \phi_1 Y_{t-1} + (\phi_2 Y_{t-2}$ or $(Y_t - \theta \epsilon_{t-1})) + \beta M_{t-k} \pm \epsilon$; where ϵ is the error term, β is the lagged regression coefficient, ϕ_i is ith order autoregessive coefficent, and θ is the moving average coefficent. This would constitute an ARMA model with a lagged independent regressor.

10. Since LERO is thought to mimic the serial behaviour of LEWL, then a model of the form: $Y_t = \phi_1 Y_{t-1} + (\phi_2 Y_{t-2}$ - if needed) $+ \beta M_{t-k} \pm \epsilon$; where ϵ is the error term, β is the lagged regression coefficient, and ϕ_i is ith order autoregessive coefficent, should best describe the relationship between MEI and LERO.

5.0 Methodology

5.1 Data Collection

The data components statistically analyzed in this research have been obtained from two primary sources. The entire Lake Erie datum (lake levels, net basin supplies, and flows of water) was supplied courtesy of Environment Canada - Great Lakes/St. Lawrence Study Office (Cornwall, Ont.). The initial MEI data set came from the NOAA-CIRES Climate Diagnostics Center, and in particular, Klaus Wolter. To make note of, the Lake Erie datum totals were averaged out from a network of gauging stations, which included Fairport, Ohio, Port Colbourne, Ont., Port Stanley, Ont., and Toledo, Ohio. All of the data was converted into a quarterly time series format, whereby an average value for each quarter was obtained by dividing the given variable's aggregate sum of the three months by 3 (e.g. Q_1 value = (Jan + Feb + Mar)/3). Each series runs from 1950 to 1998 (note- Wolter's MEI data initializes in 1950; as a result, this research begins each time series at 1950).

5.2 Methodology

To compare the serial dynamics of a) Lake Erie water levels with the Multivariate ENSO Index (MEI); b) Lake Erie net basin supply with MEI; and c) Lake Erie inflows and outflows with MEI, the data sets have been standardized on a quarterly basis (i.e. quarter 1 = Jan -Mar, quarter 2 = Apr-Jun, quarter 3 = Jul-Sep, quarter 4 = Oct-Dec) for the purpose of converting each variable into a dimensionless parameter, whereby the effects of the different units of measurement in the variable sets are removed. To convert the data to standard scores (Z), the following formula is used:

$$Z = X - \mu/\sigma$$

where X is a variate score, μ is the data mean, and σ is the standard deviation.

Box-Jenkins ARIMA (autoregressive integrated moving average) models assume that a time series is stationary, whereby the transfer function - the operation that links the input and output, cause and effect, or stimulus and response of a process or system (Bennett, 1979), remains

constant in time. If the transfer function varies as a function of time. then the series is said to be non-stationary (Bennett, 1979). To achieve a stationary time series, the following properties must be present (as presented by Chatfield, 1975):

1. there is an absence of a systematic change in mean (i.e. there is no trend),
2. there is an absence of a systematic change in variance; can be evaluated by using a test for homogeneity of variance
3. there are no significant deterministic periodic variations. and
4. the autocorrelation function (depicted on correlograms) is dependent upon the lag interval (a set time interval) and not the starting position in the time series.

Since Box-Jenkins time series techniques require stationarity within a series. the variables were tested on an individual basis for variance of the transfer function over time. Only the net basin supply (NBS) time series exhibited relative stationarity. The other four variables (LEWL. MEI. LSCO. and LERO) required interrupted time series analysis to split the series to a more desirable level of stationarity. Each series was intervened at case number 92 (1972.04), in relation to the fluctuations in the respective time series.

Once the variables were tested and found to be stationary. Box-Jenkins time series techniques were utilized to analyze the temporal behaviour of the variables. and their temporal inter-relationships with each other. Chatfield (1975) and LaValle et al. (1999) have discussed the time series procedures employed in this research. and they involve:

1. constructing correlograms depicting serial autocorrelation coefficients on one axis and their corresponding lag intervals on another (for each variable).
2. producing partial correlograms depicting the partial autocorrelation coefficients for each of the variables at each lag interval.
3. examining the observed configurations in the correlograms and partial correlograms in order to fit the data to either an autoregressive model or a moving averages model.

4. testing the residuals from the fitted models for serial autocorrelation on correlograms. This is done to assess the goodness-of-fit of the applied models.
5. cross-correlating the Lake Erie variables with MEI, in order to establish the best lag value to use with MEI in the ARIMA with regressors models.
6. constructing a series of ARIMA models with lagged values of MEI as an independent regressor in order to assess the relationship between MEI and the serial behaviour of the Lake Erie water balance variables.

5.3 The Box-Jenkins Approach vs. Spectral Analysis

Spectral analysis is the method of estimating the spectral density function, or spectrum, of a given time series. The spectral density function is a natural tool for considering the frequency properties of a time series. For example, when dealing with a purely indeterministic discrete stationary process, the spectral distribution function (refer to Chatfield (1975), p.111-116 for definition and explanation) is a continuous function in $(0, \pi)$, and can be differentiated with respect to ϖ in $(0, \pi)$. The spectral density function can be defined by the following equation:

$$f(\varpi) = dF(\varpi)/d\varpi$$

where ϖ represents the frequency of the periodic variation (i.e. number of radians per unit time), and $F(\varpi)$ represents the continuous function (Chatfield, 1975).

Spectral analysis is mainly concerned with purely indeterministic processes, which have a continuous spectrum, but can also be used for deterministic processes to pick out periodic components in the presence of noise (Chatfield, 1975). Since this research deals indirectly with climatic/weather patterns that are considered to be stochastic in nature, and as such, do not behave in a continuous manner, Box-Jenkins analysis is preferred. Also, Chatfield (1975) has stated that spectrum analysis is not used for identifying an appropriate ARIMA process; identification is an essential statistical component to this research. A third reason for choosing the Box-Jenkins approach over spectral analysis is that the latter is most useful for series with no obvious trend or 'seasonal' variation. Box-Jenkins techniques allow for seasonal components to be included into the

modeling procedures. This research deals with quarterly time series data, which contain trends and seasonal components, therefore requiring the Box-Jenkins time series modeling approach.

6.0 Results

The time series plots of the Lake Erie variables and MEI are shown in Figures 6-10. These plots clearly show why the variables LEWL, LSCO, and LERO all required to be intervened near the mid-way point of their respective series in order to achieve relative stationarity. Case number 92, which occurs during the peak of a major El Niño event, was selected for the intervention analysis. The MEI time series plot (Figure 7) shows a presence of seasonal effects - which was explored when modeling the temporal behaviour of the variable. Lake Erie net basin supply (see Figure 8) was the only variable that exhibited relative stationarity within its series.

ACF and PACF correlograms (refer to Figures 11-20) were constructed to determine the temporal behaviour of the variables. The LEWL autocorrelation function (Figure 11) shows the presence of an AR (1) process (the PACF backs this up - Figure 12), whereby the effects of the random shock to the system are still being felt well after initialization (at lag 1), but are declining in strength over time (refer to ACF correlations). The MEI correlograms (Figures 13 and 14) show significant temporal autocorrelation at lags 1 and 2, while the autocorrelation function correlogram (Figure 13) also shows a presence of seasonality (examine lags 1-10 in particular) within the system. The net basin supply correlograms (Figures 15-16) reveal no significant autocorrelation within the module, with the exception at lag 1 (note - Figure 15 shows slight autocorrelation at lag 15, Figure 16 does not). The temporal behaviour of LSCO is shown in Figures 17 and 18. The autocorrelation function of LSCO reveals the characteristics of a first-order autoregressive process. However, the partial autocorrelation function (Figure 18) shows that a first-order moving average process may also exist within the LSCO temporal model. The Lake Erie outflow temporal pattern (refer to Figures 19 and 20) shows similar behaviour to LEWL, as expected. An AR (1) process is evident, as the lags diminish in strength over time (the ACF of LERO clearly shows this effect).

Based on the observed configurations in the ACF and PACF correlograms, each variable was fit to an ARIMA model using Statistica '99. Each series, with the exception of the NBS time

Figure 6. A Time Series Plot of Standardized Lake Erie Water Levels

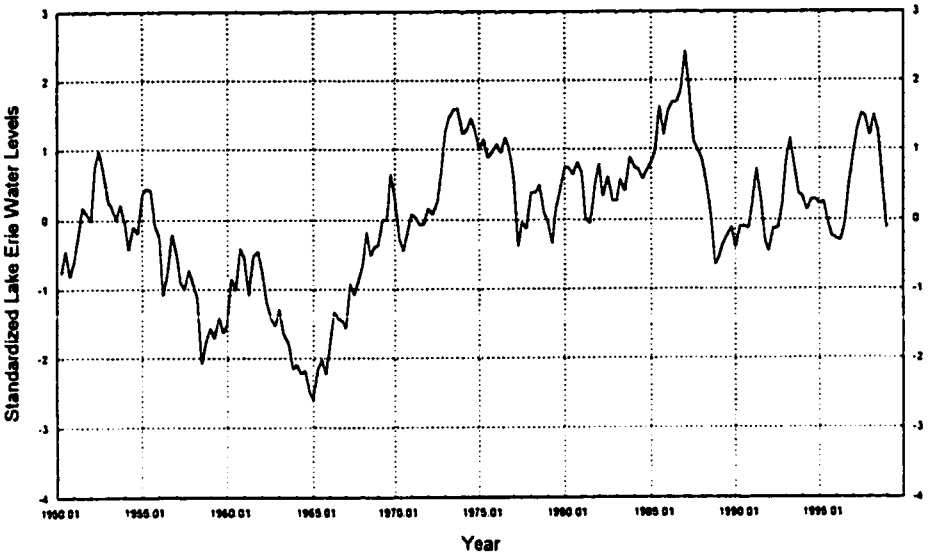

Figure 7. A Time Series Plot of the Multivariate ENSO Index

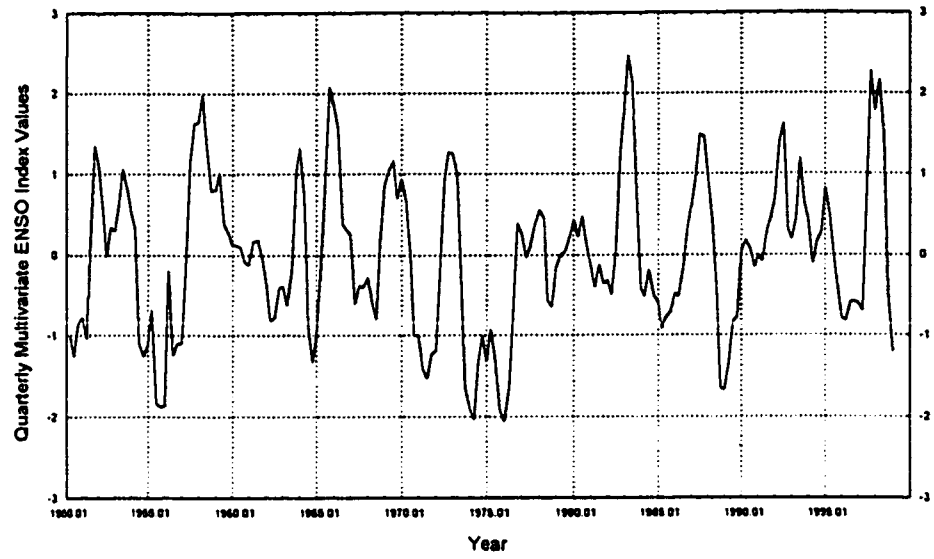

Figure 8. A Time Series Plot of Standardized Lake Erie Net Basin Supply

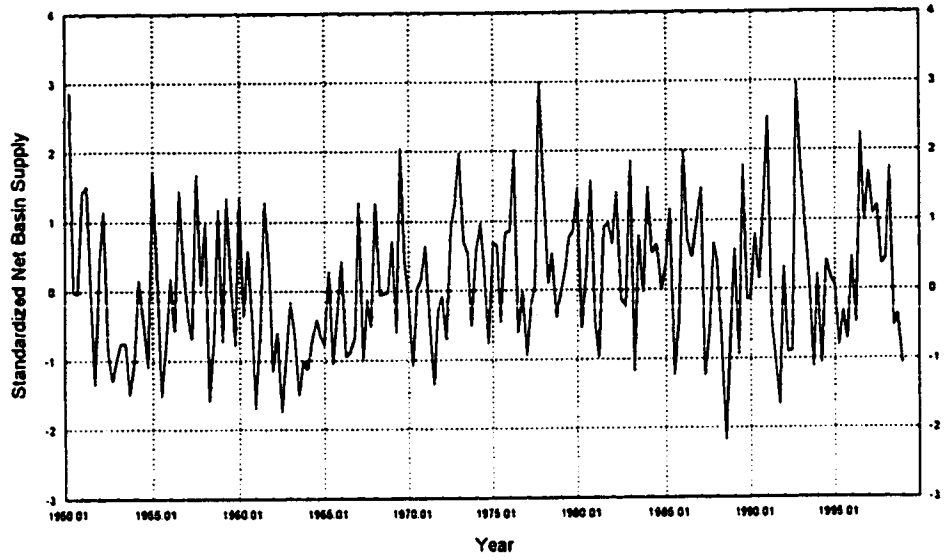

Figure 9. A Time Series Plot of Standardized Lake St. Clair Outflow

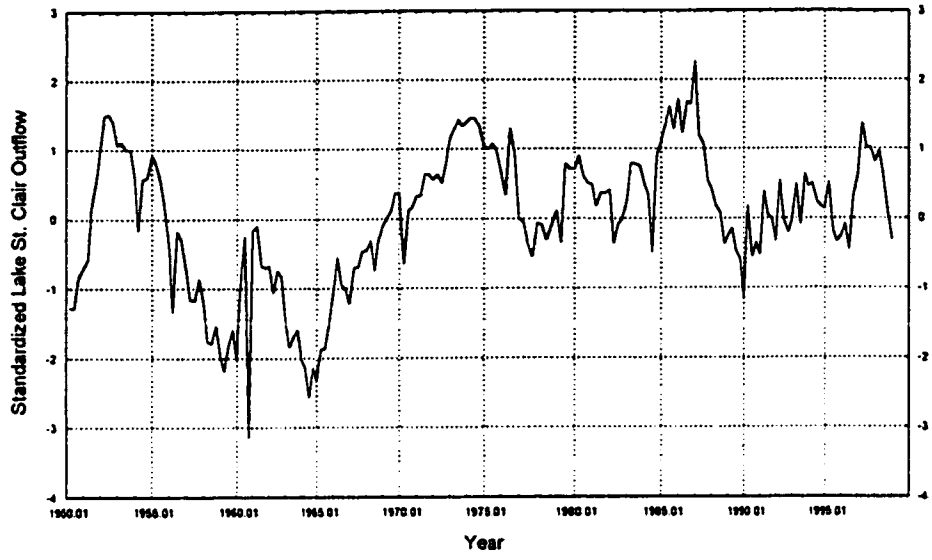

Figure 10. A Time Series Plot of Standardized Lake Erie Outflow

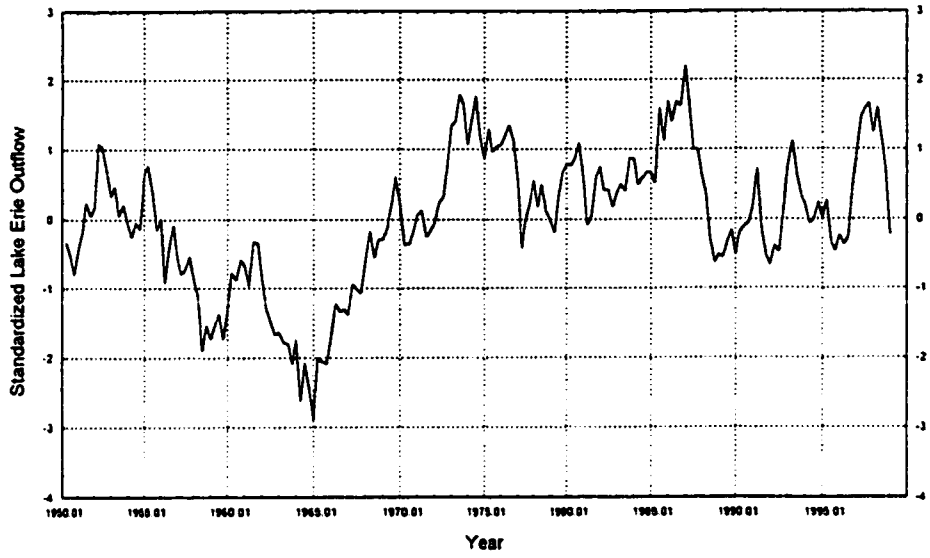

Figure 11. Autocorrelation Function
Standardized Lake Erie Water Levels
(Standard errors are white-noise estimates)

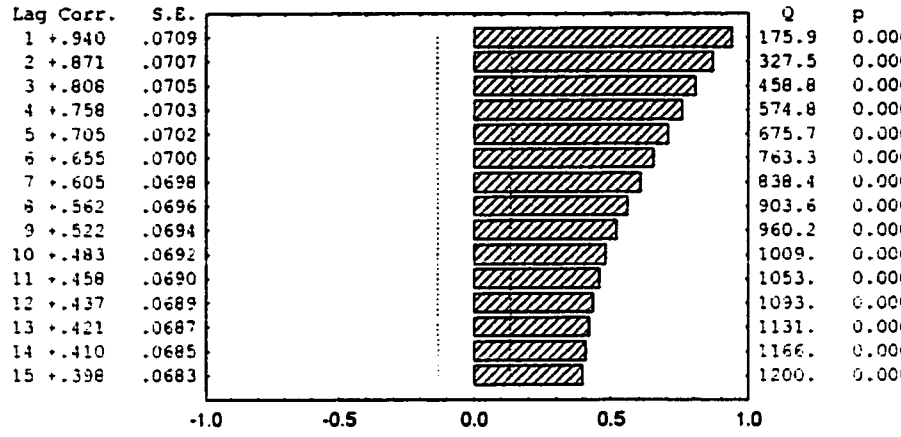

Lag	Corr.	S.E.	Q	p
1	+.940	.0709	175.9	0.000
2	+.871	.0707	327.5	0.000
3	+.808	.0705	458.8	0.000
4	+.758	.0703	574.8	0.000
5	+.705	.0702	675.7	0.000
6	+.655	.0700	763.3	0.000
7	+.605	.0698	838.4	0.000
8	+.562	.0696	903.6	0.000
9	+.522	.0694	960.2	0.000
10	+.483	.0692	1009.	0.000
11	+.458	.0690	1053.	0.000
12	+.437	.0689	1093.	0.000
13	+.421	.0687	1131.	0.000
14	+.410	.0685	1166.	0.000
15	+.398	.0683	1200.	0.000

-1.0 -0.5 0.0 0.5 1.0

Corr. = Correlation; S.E. = Standard Error
Q = Box-Ljung Q statistic; p = probability value of the Q statistic

Figure 12. Partial Autocorrelation Function
Standardized Lake Erie Water Levels
(Standard errors assume AR order of k-1)

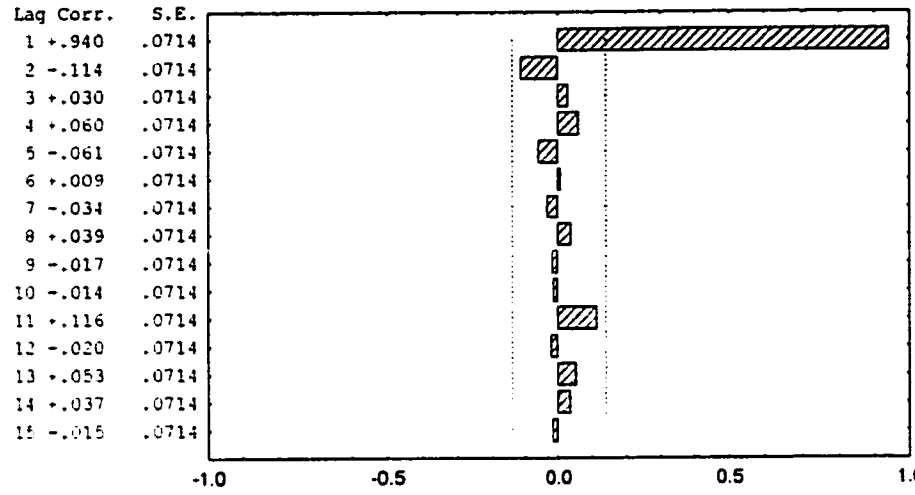

Figure 13. Autocorrelation Function

Standardized Quarterly Multivariate ENSO Index (MEI) Values

(Standard errors are white-noise estimates)

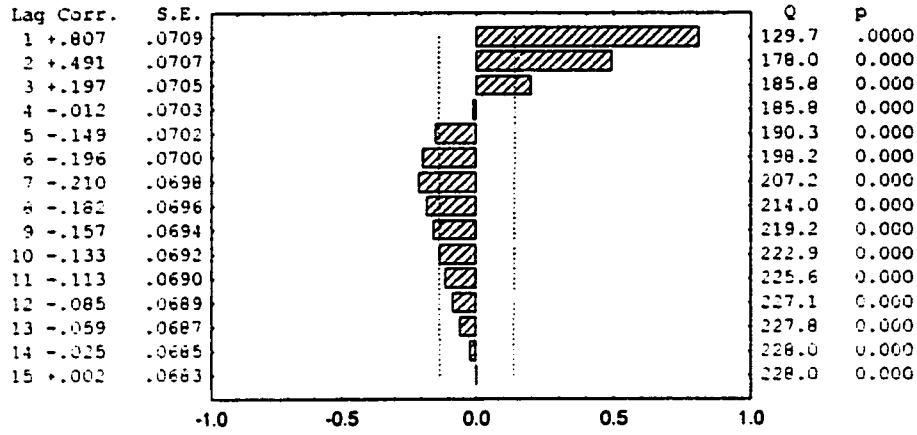

Corr. = Correlation; S.E. = Standard Error

Q = Box-Ljung Q statistic; p = probability value of the Q statistic

Figure 14. Partial Autocorrelation Function
Standardized Quarterly Multivariate ENSO Index (MEI) Values
(Standard errors assume AR order of k-1)

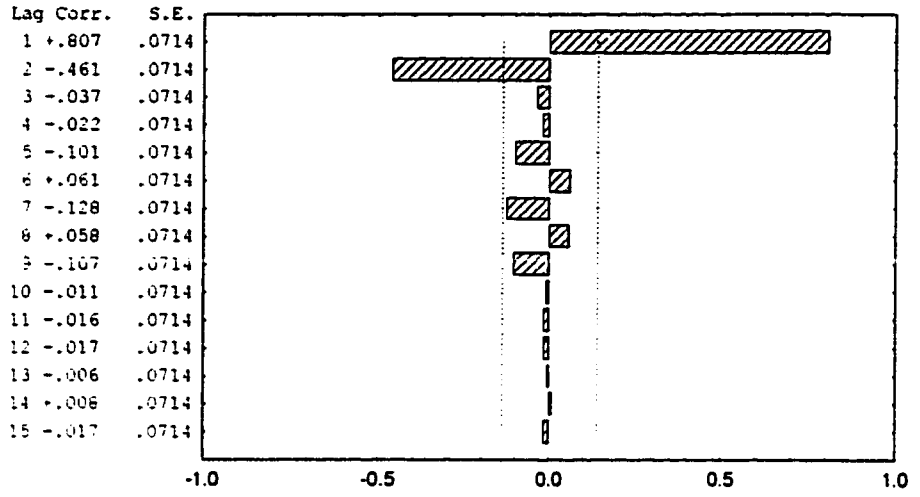

Figure 15. Autocorrelation Function

Standardized Lake Erie Net Basin Supply

(Standard errors are white-noise estimates)

Lag	Corr.	S.E.	Q	p
1	+.164	.0709	5.33	.0210
2	+.022	.0707	5.43	.0664
3	+.051	.0705	5.95	.1142
4	+.074	.0703	7.06	.1326
5	+.015	.0702	7.11	.2129
6	+.046	.0700	7.54	.2739
7	+.067	.0698	8.45	.2943
8	+.100	.0696	10.50	.2315
9	-.001	.0694	10.50	.3113
10	-.025	.0692	10.63	.3867
11	+.007	.0690	10.64	.4735
12	+.103	.0689	12.89	.3770
13	-.041	.0687	13.25	.4284
14	+.011	.0685	13.26	.5047
15	+.143	.0683	17.63	.2625

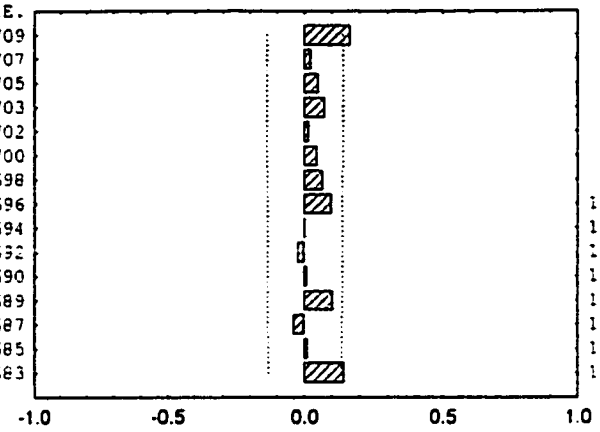

Corr. = Correlation; S.E. = Standard Error

Q = Box-Ljung Q statistic; p = probability value of the Q statistic

Figure 16. Partial Autocorrelation Function
Standardized Lake Erie Net Basin Supply
(Standard errors assume AR order of k-1)

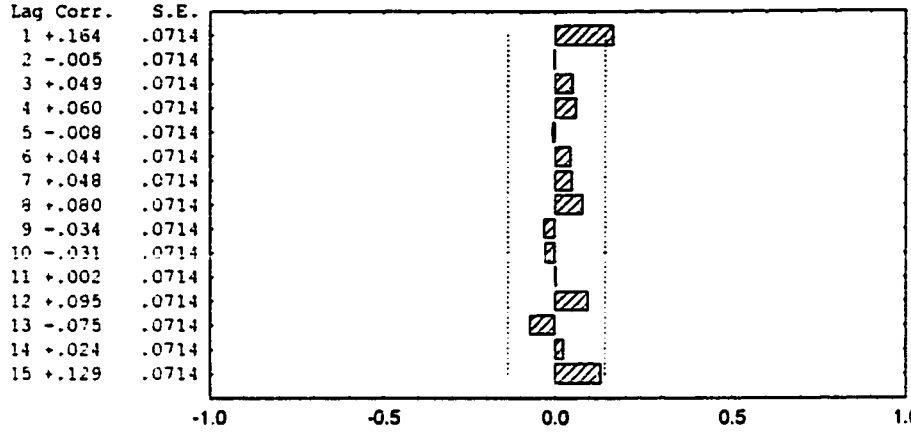

Corr. = Correlation; S.E. = Standard Error
Q = Box-Ljung Q statistic; p = probability value of the Q statistic

Figure 17. Autocorrelation Function
Standardized Lake St. Clair Outflow
(Standard errors are white-noise estimates)

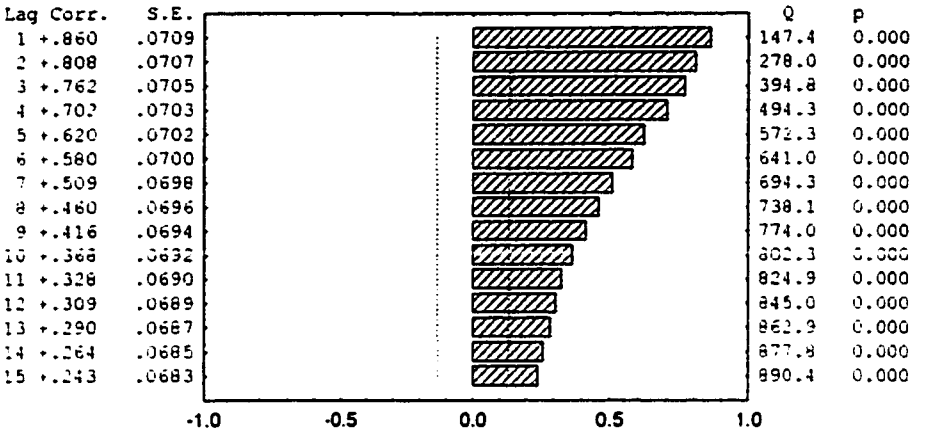

Corr. = Correlation; S.E. = Standard Error
Q = Box-Ljung Q statistic; p = probability value of the Q statistic

Figure 18. Partial Autocorrelation Function
Standardized Lake St. Clair Outflow
(Standard errors assume AR order of k-1)

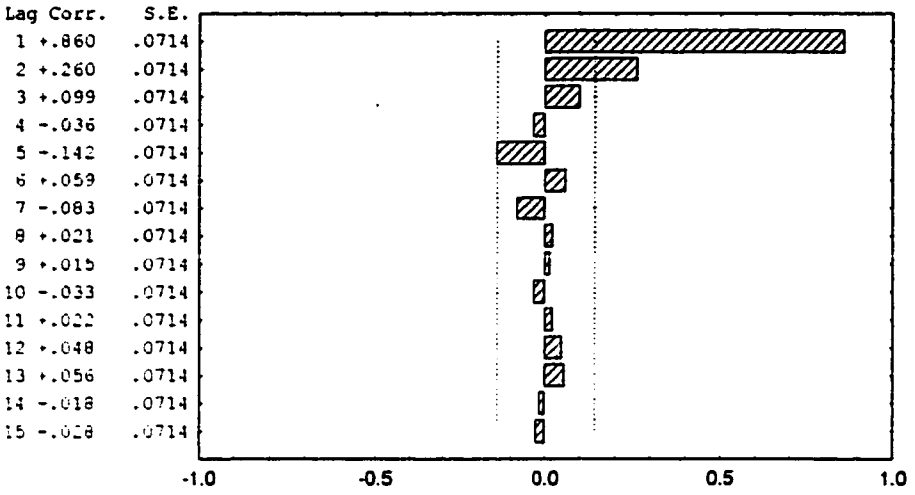

Figure 19. Autocorrelation Function
Standardized Lake Erie Outflow
(Standard errors are white-noise estimates)

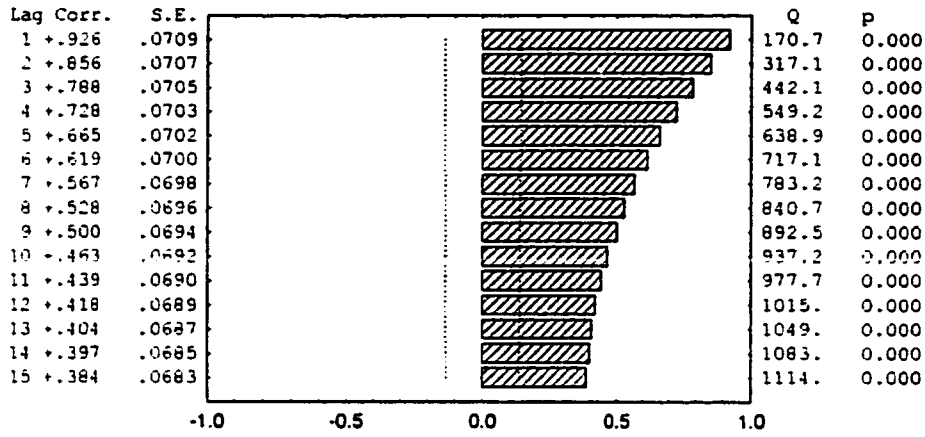

Lag	Corr.	S.E.	Q	p
1	+.926	.0709	170.7	0.000
2	+.856	.0707	317.1	0.000
3	+.788	.0705	442.1	0.000
4	+.728	.0703	549.2	0.000
5	+.665	.0702	638.9	0.000
6	+.619	.0700	717.1	0.000
7	+.567	.0698	783.2	0.000
8	+.528	.0696	840.7	0.000
9	+.500	.0694	892.5	0.000
10	+.463	.0692	937.2	0.000
11	+.439	.0690	977.7	0.000
12	+.418	.0689	1015.	0.000
13	+.404	.0687	1049.	0.000
14	+.397	.0685	1083.	0.000
15	+.384	.0683	1114.	0.000

Corr. = Correlation; S.E. = Standard Error
Q = Box-Ljung Q statistic; p = probability value of the Q statistic

Figure 20. Partial Autocorrelation Function
Standardized Lake Erie Outflow
(Standard errors assume AR order of k-1)

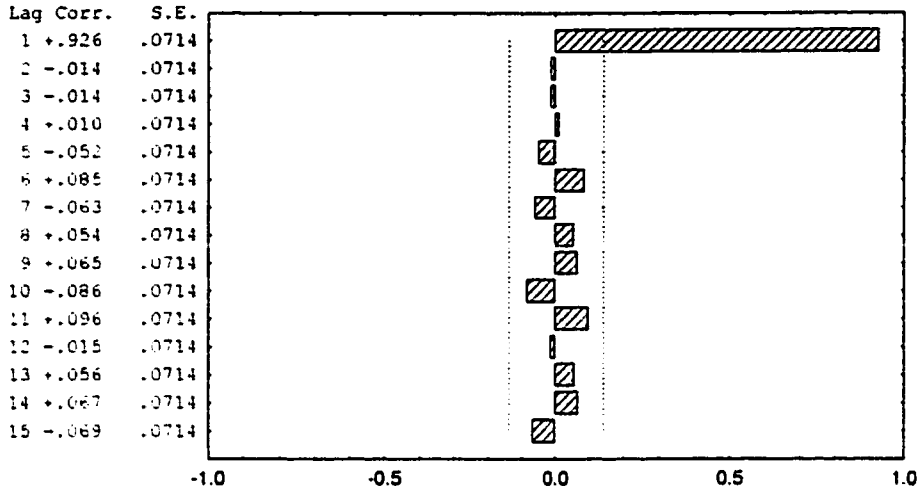

series, were subjected to intervention analysis based on the time series plots of the variables. For each variable, the most parsimonious and appropriate model fits were selected (see Figures 21, 23-26). There were no significant autocorrelations in the correlograms of the residuals, as indicated by the probabilities associated with the Box-Ljung Q statistics.

6.1 Lake Erie Water Levels

Lake Erie water levels (LEWL) were fit to a first-order (1,0,0) autoregressive model. Table 3 highlights the appropriateness of the model fit. The p (1) autoregressive parameter has a high estimation value of .93, while the Om intervention estimation is significant at .57. The (1,0,0) model explains 88.63% of the variations within the series. The autocorrelation function of the residuals (Figure 21) shows no observable significant autocorrelations. The probabilities associated with the Box-Ljung Q statistics are all well over the .05 level, indicating no significant autocorrelation in the set of residuals.

TABLE 3. LEWL TEMPORAL MODEL FIT (1, 0, 0)
Statistica '99 Output

Variable: LEWL
Transformations: None
Model: (1, 0, 0) Interventions: 1
Estimation: Approximate Max. Likelihood Method (McLeod & Sales)
No. Iterations: 13
No. of obs.: 196 Initial SS = 191.97 Final SS = 21.825 (11.37%) MS = .11308
Parameters (p/PS = Autoregressive/seasonal, q/Qs = Moving average/seasonal)

	p (1)	Om (1)
Estimate:	.92798	.57082
Std. Err.:	.02714	.27104
t (193):	34.192	2.1060
Lower 95%:	.87445	.03623
Upper 95%:	.98151	1.1054

An AR (2) model has been constructed to show that a second-order autoregressive process is an inadequate descriptor of the serial behaviour of LEWL (refer to Table 4). The p (1) autoregressive parameter estimate is over the value of 1, indicating that the model may be non-stationary or non-invertible. The p (2) autoregressive parameter is non-significant at -.1134, which

indicates that this model has been over-identified. Although approximately 89% of the variations within the series can be accounted for with the AR (2) model - marginally better than the AR (1) model, the model must be rejected because it has over-identified the temporal process of Lake Erie water levels. Figure 22, the residual correlogram of the model fit, appears to reveal a good fit with the AR (2) model. However, since the p (2) parameter is insignificant in the model fit, the residuals of the AR (2) model fit are irrelevant.

TABLE 4. LEWL TEMPORAL MODEL FIT (2, 0, 0)
(Statistica '99 Output)

Variable: LEWL
Tansformations: None
Model: (2, 0, 0) Interventions: 1
Estimation: Approximate Max. Likelihood Method (McLeod & Sales)
No. Iterations: 16
No. of obs.: 196 Initial SS = 191.97 Final SS = 21.553 (11.23%) MS = .11226
Parameters (p/Ps = Autoregressive/seasonal, q/Qs = Moving average/seasonal)

	p (1)	p (2)	Om (1)
Estimate:	1.0032	-.1134	.52874
Std. Err.:	.07290	.07285	.26118
t (192):	14.174	-1.556	2.0244
Lower 95%:	.88946	-.2571	.01359
Upper 95%:	1.1770	.03032	1.0439

Since the LEWL model contains a first-order autoregressive process, hypothesis #3 can be accepted. The results here re-enforce the findings of LaValle et al. (1999), that standardized Lake Erie water level fluctuations are associated with a long memory stochastic process. Kite's (1992) findings that Lake Erie water levels can be associated with a second-order autoregressive process can not be further validated by the results here, and as such, hypothesis #2 must be rejected. It may be important to note that Kite used spectral analysis with monthly data to achieve his results. This may help to explain why differences in Lake Erie water level models exist between the results of this research (and/or LaValle et al., 1999) and Kite (1992).

Figure 21. Autocorrelation Function

Lake Erie Water Level Residuals From An AR (1) Model

Intervention Analysis at Case Number 92

(Standard errors are white-noise estimates)

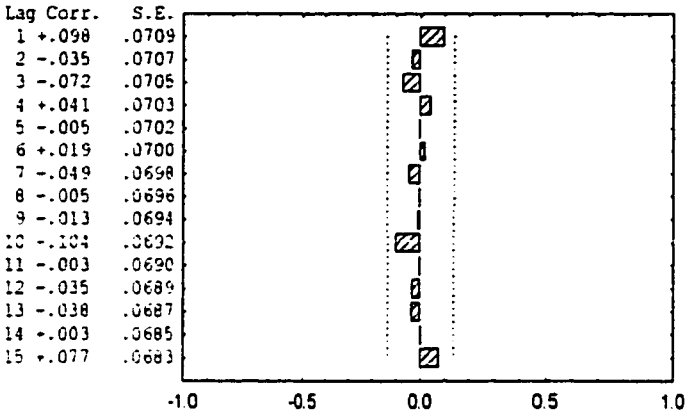

Lag	Corr.	S.E.	Q	p
1	+.098	.0709	1.92	.1662
2	-.035	.0707	2.16	.3390
3	-.072	.0705	3.22	.3595
4	+.041	.0703	3.56	.4683
5	-.005	.0702	3.57	.6130
6	+.019	.0700	3.64	.7247
7	-.049	.0698	4.13	.7649
8	-.005	.0696	4.13	.8449
9	-.013	.0694	4.17	.9002
10	-.104	.0692	6.42	.7791
11	-.003	.0690	6.42	.8439
12	-.035	.0689	6.68	.8782
13	-.038	.0687	6.99	.9027
14	+.003	.0685	6.99	.9350
15	+.077	.0683	8.25	.9133

Corr. = Correlation; S.E. = Standard Error

Q = Box-Ljung Q statistic; p = probabilty value of the Q statistic

Figure 22. Autocorrelation Function

Lake Erie Water Level Residuals From An AR (2) Model

Intervention Analysis at Case Number 92

(Standard errors are white-noise estimates)

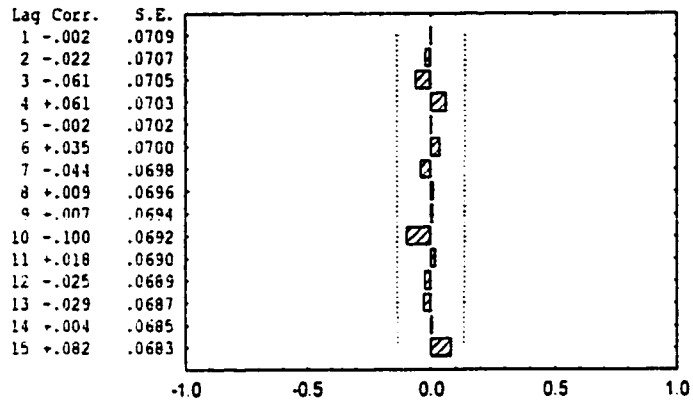

Lag	Corr.	S.E.	Q	p
1	-.002	.0709	.00	.9816
2	-.022	.0707	.10	.9527
3	-.061	.0705	.83	.8414
4	+.061	.0703	1.59	.8109
5	-.002	.0702	1.59	.9026
6	+.035	.0700	1.84	.9336
7	-.044	.0698	2.24	.9456
8	+.009	.0696	2.25	.9723
9	-.007	.0694	2.26	.9866
10	-.100	.0692	4.33	.9314
11	+.018	.0690	4.39	.9570
12	-.025	.0689	4.53	.9719
13	-.029	.0687	4.71	.9811
14	+.004	.0685	4.71	.9895
15	+.082	.0683	6.17	.9768

Corr. = Correlation; S.E. = Standard Error

Q = Box-Ljung Q statistic; p = probability value of the Q statistic

6.2 The Multivariate ENSO Index

The Multivariate ENSO Index time series best fit an ARMA model of (1,0,0) (1,0,0), with a seasonal lag of 5. The appropriateness of the model fit is highlighted in Table 5. The p (1), q (1), and P (s) parameters were are all significant, while the Om parameter was an insignificant factor - which indicates that this series did not require to be split at case number 92. The ARMA (1,0,0) (1,0,0) model fit explains 72.75% of the variations in the serial behaviour of MEI. An examination of the residual autocorrelation function (Figure 23) demonstrates that all of the autocorrelations fall inside of the 5 percent confidence bands, with the exception at lag 3, and that all of the probabilities (p) associated with the Box-Ljung Q statistics are greater than 0.05. Slight autocorrelation exists at lag 3, which can be dismissed as marginal error within the system. These results support the ARMA (1,0,1) (1,0,0) model as being an adequate descriptor of MEI serial behaviour.

TABLE 5. MEI TEMPORAL MODEL FIT
(Statistica '99 Output)

Variable: MEI
Transformations: None
Model: (1, 0, 1) (1, 0, 0) Season: 5 Interventions: 1
Estimation: Approximate Max. Likelihood Method (McLeod & Sales)
No. Iterations: 19
No. of obs: 196 Initial SS = 182.63 Final SS = 49.758 (27.25%) MS = .26052
Parameters (p/Ps = Autoregressive/seasonal. q/Qs = Moving average/seasonal)

	p (1)	q (1)	Ps (1)	Om (1)
Estimate:	.70853	-.4315	-.2274	-.0418
Std. Err.:	.05661	.06371	.07351	.18584
t (191):	12.515	-6.772	-3.094	-.2252
Lower 95%:	.59686	-.5571	-.3724	-.4084
Upper 95%:	.82019	-.3058	-.0824	.32471

The model found here provides evidence of psuedo-cyclic behaviour within the MEI time series. The significance of both long-term and short-term effects in the serial behaviour of MEI implies that stochastic forcing may be influencing the ENSO cycles, but probably on a different time scale for El Niño and La Niña occurrences. However, a seasonal autoregressive process of 15

Figure 23. Autocorrelation Function

Quarterly Multivariate ENSO Index Residuals From An ARMA (1,0,1) (1,0,0) Model

Intervention Analysis at Case Number 92; Seasonal Lag of 5

(Standard Errors are white-noise estimates)

Lag	Corr.	S.E.	Q	p
1	+.018	.0709	.07	.7954
2	+.118	.0707	2.84	.2413
3	-.150	.0705	7.36	.0612
4	-.029	.0703	7.53	.1102
5	-.007	.0702	7.54	.1832
6	-.047	.0700	7.99	.2390
7	-.052	.0698	8.54	.2870
8	-.076	.0696	9.73	.2847
9	-.035	.0694	9.99	.3516
10	+.005	.0692	9.99	.4413
11	-.066	.0690	10.89	.4523
12	-.032	.0689	11.11	.5195
13	-.107	.0687	13.54	.4069
14	+.030	.0685	13.73	.4700
15	+.066	.0683	14.66	.4758

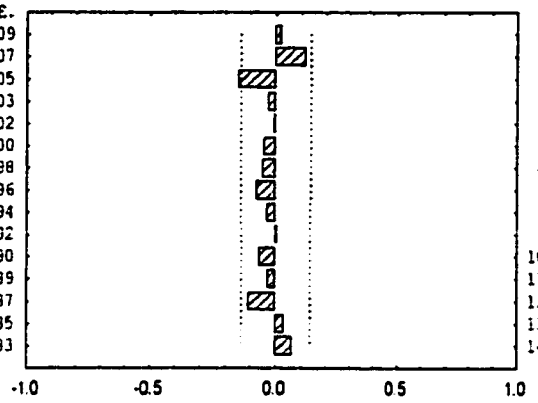

Corr. = Correlation; S.E. = Standard Error

Q =Box-Ljung Q statistic; p = probability value of the Q statistic

months (1.25 years) is present within the model, which does narrow down what the average length of an ENSO event or partial ENSO event may be.

6.3 Lake Erie Net Basin Supply

Lake Erie net basin supply was best fit to a first-order (1,0,0) autoregressive model (refer to Table 6 and Figure 24). Table 6 highlights the appropriateness of the model fit. Only 3% of the variations in the serial behaviour were accounted for within this model. Since there is marginal autocorrelation in the NBS time series to begin with (refer to Figure 24), it is very reasonable to expect low variation accountability. Essentially, this enforces the idea that the net basin supply of Lake Erie fluctuates more so on a random basis than on a cyclical period. Net basin supply is probably slightly autocorrelated at lag 1 because the water levels are associated with long-memory processes. Since net basin supply accounts for 13% of the total water supply of Lake Erie, it seems logical that the NBS would follow a similar temporal pattern to LEWL. However, variation of the temporal patterns should not be totally unexpected, due to this low percentage relationship between NBS and LEWL. Hypothesis #4 can be accepted, as the Lake Erie net basin supply does assume a first-order autoregressive process, albeit a weak one.

TABLE 6. LENBS TEMPORAL MODEL FIT
(Statistica '99 Output)

Variable: LENBS
Transformations: None
Model: (1, 0, 0)
Estimation: Approximate Max. Likelihood Method (McLeod & Sales)
No. Iterations: 7
No. of obs.: 196 Initial SS = 202.76 Final SS = 196.61 (96.97%) MS = 1.0134
Parameters (p/Ps = Autoregressive/seasonal, q/Qs = Moving average/seasonal)

	p (1)
Estimate:	.17471
Std. Err.:	.07090
t (194):	2.4641
Lower 95%:	.03487
Upper 95%:	.31454

Figure 24. Autocorrelation Function

Lake Erie Net Basin Supply Residuals From An AR (1) Model

(Standard errors are white-noise estimates)

Lag	Corr.	S.E.	Q	p
1	-.009	.0709	.02	.8970
2	-.015	.0707	.06	.9710
3	+.038	.0705	.35	.9512
4	+.065	.0703	1.21	.8771
5	-.006	.0702	1.21	.9435
6	+.034	.0700	1.45	.9628
7	+.044	.0698	1.84	.9682
8	+.093	.0696	3.62	.8895
9	-.016	.0694	3.67	.9315
10	-.028	.0692	3.84	.9542
11	-.009	.0690	3.86	.9739
12	+.116	.0689	6.70	.8770
13	-.065	.0687	7.59	.8694
14	-.006	.0685	7.59	.9093
15	+.135	.0683	11.50	.7162

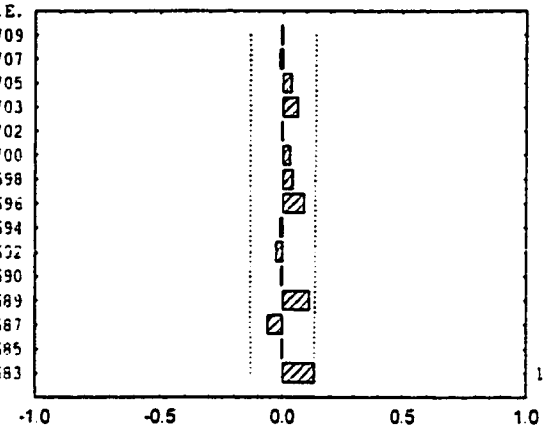

Corr. = Correlation; S.E. = Standard Error

Q = Box-Ljung Q statistic; p = probability value of the Q statistic

6.4 Lake St. Clair Outflow

An ARMA (1,0,1) model best fit the Lake St. Clair outflow data set (see Table 7 and Figure 25). Table 7 highlights the appropriateness of the model fit. The p (1) autoregressive parameter estimate is very high at .926, indicating that a strong first-order autoregressive process exists with the Lake St. Clair outflow. However, the q (1) moving average parameter is statistically significant, which means that there are points in the series where outflow rates dissipate on a more abrupt basis. Therefore, this model can be deemed to have revealed the existence of a psuedo-cyclic process within the main source of Lake Erie inflow. The reason for this may be linked to the north/south orientation of Lakes Huron and Michigan. The orientation of the connecting north/south lakes (Huron, Michigan, St. Clair) may produce similar temporal processes (due to similar wind conditions), while a predominantly west-east oriented lake (Lake Erie, in particular) may experience dampered effects to its system, due to a change in lake orientation.

TABLE 7. LSCO TEMPORAL MODEL FIT
(Statistica '99 Output)

Variable: LSCO
Transformations: None
Model: (1, 0, 1) Interventions: 1
Estimation: Approximate Max. Likelihood Method (McLeod & Sales)
No. Iterations: 19
No. of obs.: 196 Initial SS = 192.00 Final SS = 45.778 (23.84%) MS = .23843
Parameters (p/Ps = Autoregressive/seasonal, q/Qs = Moving average/seasonal)

	p (1)	q (1)	Om (1)
Estimate:	.92696	.30383	.44375
Std. Err.:	.03078	.07256	.32188
t (192):	30.115	4.1872	1.3786
Lower 95%:	.86625	.16071	-.1911
Upper 95:	.98767	.44695	1.0786

6.5 Lake Erie Outflow

Lake Erie outflow was best fit to a first-order (1,0,0) autoregressive model. Table 8 highlights the appropriateness of the model fit. Approximately 86% of the serial variation within the Lake Erie outflow data is accounted for with the AR (1) model. Figure 26, the Lake Erie

Figure 25. Autocorrelation Function

Lake St. Clair Outflow Residuals From An ARMA (1,0,1) Model

Intervention Analysis at Case Number 92

(Standard errors are white-noise estimates)

Lag	Corr.	S.E.	Q	p
1	-.017	.0709	.06	.8093
2	+.012	.0707	.09	.9574
3	+.093	.0705	1.84	.6057
4	+.065	.0703	3.32	.5062
5	-.098	.0702	5.26	.3849
6	+.075	.0700	6.41	.3794
7	-.057	.0698	7.08	.4204
8	-.029	.0696	7.26	.5089
9	-.006	.0694	7.27	.6094
10	-.060	.0692	8.02	.6267
11	-.078	.0690	9.29	.5948
12	-.013	.0689	9.33	.6747
13	+.025	.0687	9.46	.7370
14	+.003	.0685	9.47	.8000
15	+.066	.0683	10.41	.7933

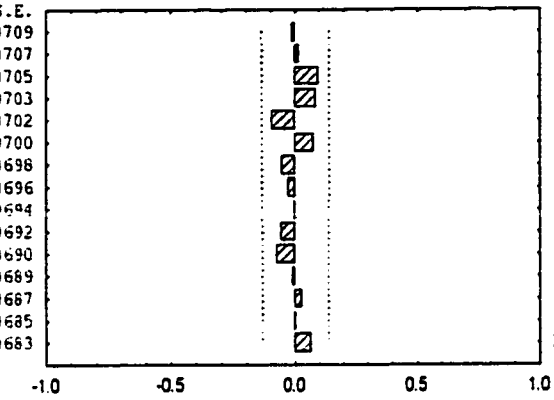

Corr. = Correlation; S.E. = Standard Error

Q = Box-Ljung Q statistic; p = probability value of the Q statistic

Figure 26. Autocorrelation Function

Lake Erie Outflow Residuals From An AR (1) Model

Intervention Analysis at Case Number 92

(Standard errors are white-noise estimates)

Lag	Corr.	S.E.	Q	p
1	+.011	.0709	.02	.8748
2	+.004	.0707	.03	.9862
3	-.015	.0705	.07	.9947
4	+.049	.0703	.55	.9681
5	-.097	.0702	2.47	.7804
6	+.055	.0700	3.10	.7966
7	-.053	.0698	3.68	.8162
8	-.064	.0696	4.51	.8081
9	+.056	.0694	5.17	.8193
10	-.076	.0692	6.37	.7835
11	+.011	.0690	6.39	.8460
12	-.034	.0689	6.64	.8806
13	-.048	.0687	7.13	.8952
14	+.039	.0685	7.46	.9153
15	+.063	.0683	8.30	.9111

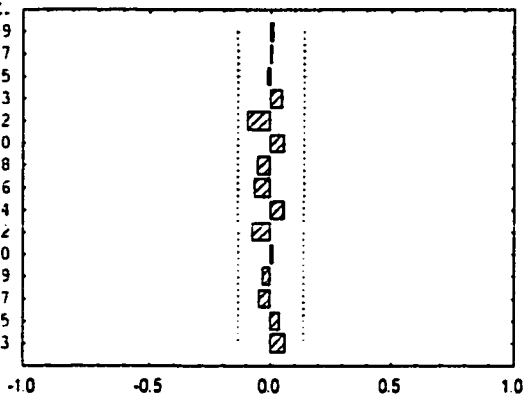

Corr. = Correlation; S.E. = Standard Error

Q = Box-Ljung Q statistic; p = probability value of the Q statistic

outflow residual correlogram, shows that no significant autocorrelations fall outside of the 5 percent confidence bands. The probability values (p) of the Box-Ljung Q statistics are quite high indicating no significant autocorrelation in the set of residuals.

TABLE 8. LERO TEMPORAL MODEL FIT
(Statistica '99 Output)

Variable: LERO
Transformations: None
Model: (1, 0, 0) Interventions: 1
Estimation: Approximate Max. Likelihood Method (McLeod & Sales)
No. Iterations: 12
No. of obs.: 196 Initial SS = 192.01 Final SS = 26.809 (13.96%) MS = .13891
Parameters (p/Ps = Autoregressive/seasonal, q/Qs = Moving average/seasonal)

	p (1)	Om (1)
Estimate:	.91310	.54375
Std. Err.:	.02968	.27897
t (193):	30.765	1.9492
Lower 95%:	.85456	-.0065
Upper 95%:	.97164	1.0940

The primary outflow of Lake Erie seems to be associated with a long-memory stochastic process, as found with Lake Erie water levels. In all likelihood, these two variables distinguish identical (or near identical) serial behaviour because of the same axis-orientation.

6.6 Cross-Correlations

Using the statistical computer software program Statistica '99 (Statsoft, 1999), cross-correlation function correlograms were constructed to depict any possible relationships between the Lake Erie variables (LEWL, NBS, LSCO, and LERO) and the Multivariate ENSO Index (MEI). Figure 27 illustrates a cross-correlogram describing the serial relationships between LEWL and MEI. There are notable significant correlations at lags 4, 5, 13, and 14. Lag 14, is of particular interest, since it exhibits the highest correlation (r = .169) between the two variables. A such, a 3 1/2 year (weak) relationship between LEWL and MEI will be tested for in an independent regressor ARMA model. Note - the negative lag correlations depicted between LEWL and MEI are irrelevant and illogical, because they give the meaning that the Multivariate ENSO Index follows the LEWL parameter, rather than preceding it. Figure 28 shows that there is a

Figure 27. Cross-Correlation Function
Standardized Lake Erie Water Levels
Lagged: Quarterly Multivariate ENSO Index Values

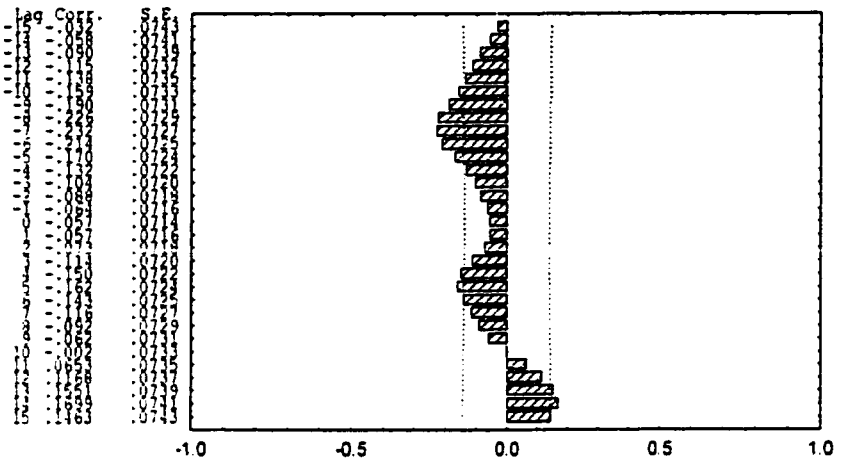

Corr. = Correlation; S.E. = Standard Error

Figure 28. Cross-Correlation Function
Standardized Lake Erie Net Basin Supply
Lagged: Quarterly Multivariate ENSO Index Values

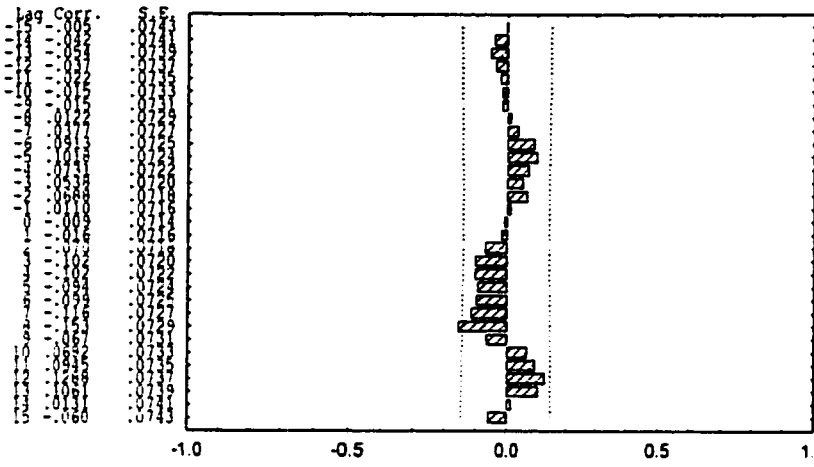

Corr. = Correlation; S.E. = Standard Error

Figure 29. Cross-Correlation Function
Standardized Lake St. Clair Outflow
Lagged: Quarterly Multivariate ENSO Index Values

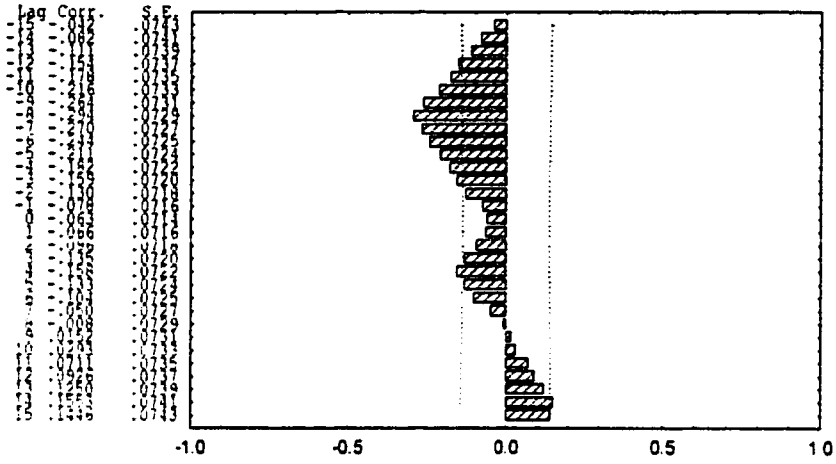

Corr. = Correlation; S.E. = Standard Error

Figure 30. Cross-Correlation Function
Standardized Lake Erie Outflow
Lagged: Quarterly Multivariate ENSO Index Values

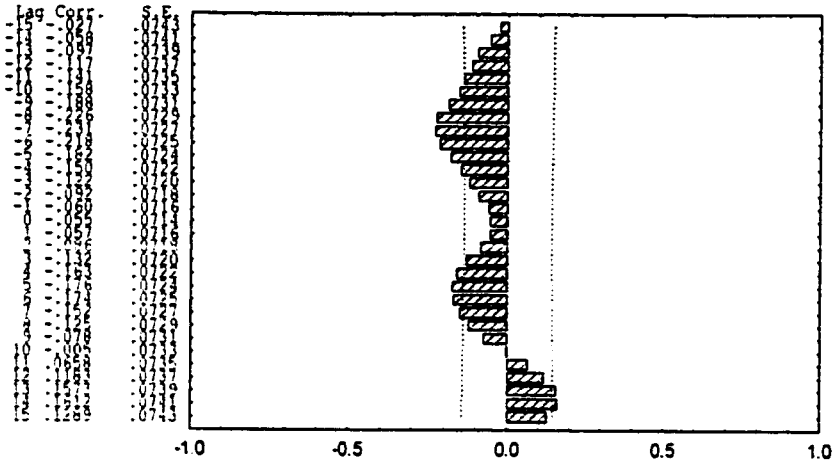

Corr. = Correlation; S.E. = Standard Error

significant correlation at lag 8 between Lake Erie net basin supply and MEI (r = -.153). This lag period will be used in an independent regressor ARMA model to assess the possibility of a weak, inverse relationship between LENBS and MEI. Lake St. Clair outflows cross-correlated with MEI (see Figure 29) reveal that significant relationships may exist at lags 4 (1 year; r = -.158) and 14 (3 1/2 years; r = .155). However, since Lake Erie net basin supply may have a possible relationship with ENSO after a 2 year time period, it is more than likely that the lag 4 correlation will not be an adequate temporal relationship descriptor of LSCO and MEI. Subsequently, a 3 1/2 year, weak, direct relationship between LSCO and MEI will be tested for in an ARMA (1, 0, 1) regression model. Figure 30 illustrates a cross-correlogram describing the serial relationships between LERO and MEI. There are significant correlations at lags 4-7, and lags 13-14. As with LEWL and LSCO, the significant negative lag correlations have been discarded as being illogical. Since LERO relatively mimics the temporal behaviour of LEWL, a 3 1/2 year, weak, direct lagged relationship (r = .161) between LERO and MEI will be tested for in an independent regressor ARMA model.

6.7 ARMA With Lagged Regressors Models of Lake Erie Hydrologic Parameters

6.7.1 The LEWL-MEI Model

When the Lake Erie water level data was put into an ARMA model with lagged values of MEI as an independent regressor, an AR (1) model with MEI lagged 3 1/2 years (lag = 14 quarters) produced the best results, as the model accounted for 89% of the serial variation in LEWL (see Table 9 and Figure 31). No significant autocorrelation was observed in the residuals from this model as evidenced by the non-significant Box-Ljung statistics. If one used the regression approach of Quinn and Guerra (1986), a higher proportion of the variance in the system could be explained, but some question would remain as to the presence of autocorrelation in the system. If such data are not available or if one wishes to forecast the near future water levels, the model presented in this research would be more elegant, less data dependent, and still yield a high level of predictive power.

Figure 31. Autocorrelation Function
LEWL/MEI Residuals From An AR (1) Model
Independent Regressor: MEI - 3 1/2 Year Lag
(Standard errors are white-noise estimates)

Lag	Corr.	S.E.	Q	p
1	+.085	.0735	1.33	.2486
2	-.064	.0733	2.09	.3518
3	-.086	.0731	3.48	.3236
4	+.074	.0729	4.50	.3426
5	+.051	.0727	4.99	.4173
6	+.050	.0725	5.46	.4862
7	-.054	.0723	6.03	.5366
8	+.047	.0721	6.44	.5977
9	+.013	.0719	6.47	.6917
10	-.106	.0717	8.67	.5637
11	-.027	.0715	8.81	.6394
12	-.040	.0712	9.12	.6926
13	-.061	.0710	9.85	.7058
14	+.037	.0708	10.13	.7529
15	+.063	.0706	11.52	.7150

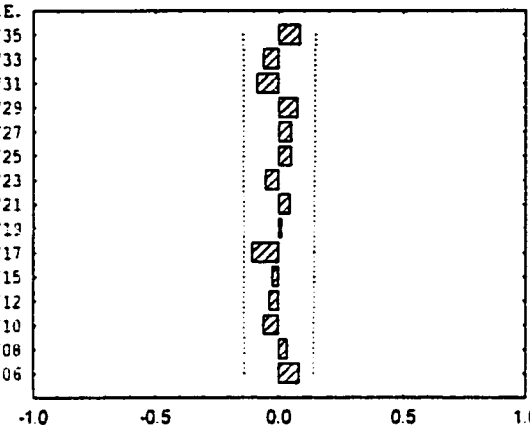

Q = Box-Ljung Q statistic; p = probability value of the Q statistic

TABLE 9. MODEL OF LAKE ERIE WATER LEVELS AND MEI

	B	SEB	T-RATIO	APPROX. PROB.
AR1	.94123171	.02404271	39.148324	.00000000
MEIQ14	.12932143	.04407872	2.933874	.00378348

(R^2 = .893)

6.7.2 The LENBS-MEI Model

With MEI lagged (8 quarters) as an independent regressor against Lake Erie net basin supply in an AR (1) model, a weak but significant relationship was found to exist (see Table 10). There were no significant autocorrelations observed in the residuals from this model, as evidenced by the non-significant Box-Ljung Q statistics (see Figure 32). Approximately 5% of the serial variation in LENBS was accounted for with this model, which means that random, temporal behaviour is probably predominant with net basin supply. The exception to this occurs when initial shocks are felt in the system, which tend to exhibit declining marginal autocorrelation over time.

TABLE 10. MODEL OF LAKE ERIE NET BASIN SUPPLY AND MEI

	B	SEB	T-RATIO	APPROX. PROB.
AR1	.17183444	.07225792	2.3780705	.01841710
ZMEI8	-.19839581	.08800778	-2.2542984	.02534368

(R^2 = .047)

6.7.3 The LSCO-MEI Model

When the Lake St. Clair outflow data was fitted to an ARMA (1,0,1) model with lagged MEI values (lag = 14 quarters) as an independent regressor variable, significant results were obtained, while 77.6% of the serial variation in LSCO was accounted for. The combined model is depicted in Table 11, with the residuals for this model depicted in Figure 33.

Figure 32. Autocorrelation Function
LENBS/MEI Residuals From An AR (1) Model
Independent Regressor: MEI - 2 Year Lag
(Standard errors are white-noise estimates)

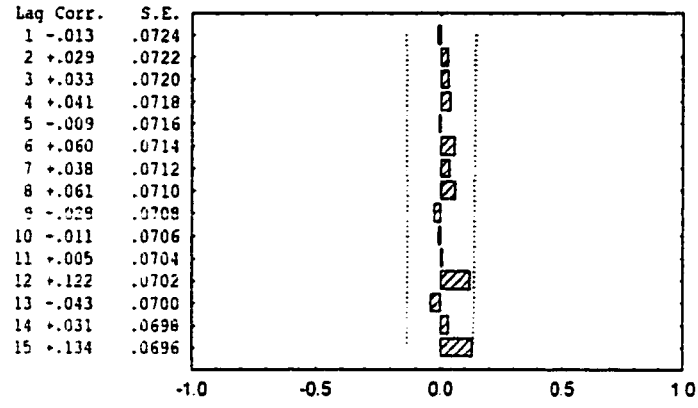

Lag	Corr.	S.E.	Q	p
1	-.013	.0724	.03	.8556
2	+.029	.0722	.19	.9096
3	+.033	.0720	.41	.9392
4	+.041	.0718	.74	.9466
5	-.009	.0716	.75	.9800
6	+.060	.0714	1.46	.9621
7	+.038	.0712	1.74	.9727
8	+.061	.0710	2.49	.9621
9	-.029	.0708	2.65	.9767
10	-.011	.0706	2.67	.9881
11	+.005	.0704	2.68	.9943
12	+.122	.0702	5.69	.9309
13	-.043	.0700	6.07	.9434
14	+.031	.0698	6.27	.9593
15	+.134	.0696	9.99	.8205

Corr. = Correlation; S.E. = Standard Error
Q = Box-Ljung Q statistic; p = probability value of the Q statistic

Figure 33. Autocorrelation Function

LSCO/MEI Residuals From An ARMA (1, 0, 1) Model

Independent Regressor - MEI 3 1/2 Year Lag

(Standard errors are white-noise estimates)

Lag	Corr.	S.E.	Q	p
1	-.029	.0735	.15	.6964
2	-.011	.0733	.17	.9167
3	+.085	.0731	1.54	.6735
4	+.143	.0729	5.41	.2482
5	-.087	.0727	6.85	.2324
6	+.074	.0725	7.89	.2460
7	-.037	.0723	8.16	.3192
8	+.026	.0721	8.28	.4066
9	+.002	.0719	8.28	.5061
10	-.065	.0717	9.10	.5230
11	-.079	.0715	10.33	.5009
12	-.023	.0712	10.43	.5782
13	-.006	.0710	10.44	.6577
14	-.001	.0709	10.44	.7294
15	+.050	.0706	10.93	.7575

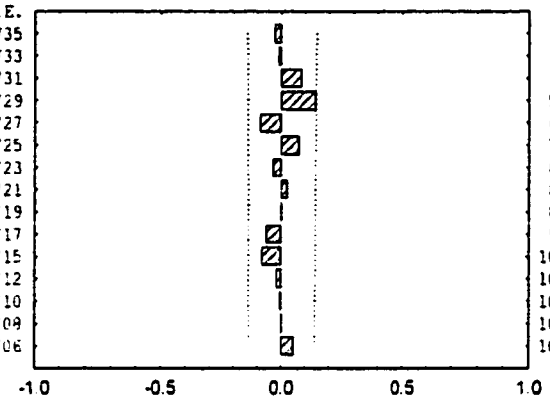

Corr. = Correlation; S.E. = Standard Error

Q = Box-Ljung Q statistic; p = probability value of the Q statistic

TABLE 11. MODEL OF LAKE ST. CLAIR OUTFLOWS AND MEI

	B	SEB	T-RATIO	APPROX. PROB.
AR1	.95028648	.02472962	38.427049	.00000000
MA1	.40393319	.07715428	5.235396	.00000046
MEIQ14	.15363506	.05274204	2.912953	.00403660

(R^2 = .776)

Judging from these results, and the LSCO-MEI cross-correlation correlogram (Figure 29) it does not appear that the influence of MEI is stronger with Lake St.Clair outflow, as previously suggested (refer back to hypothesis # 9). These results indicate that water in the upper lakes may not be as strongly affected by ENSO conditions as originally thought. The deeper water systems may actually prevent ENSO events from significantly altering the water balance of the upper lakes. Of course, this is merely speculation, and as such, until research on the upper Great Lakes region has been completed and accepted as being scientifically sound, no definitive conclusions can be made on the subject matter.

6.7.4 The LERO-MEI Model

When the Lake Erie outflow data were fitted to an ARMA model with lagged MEI values as an independent regressor variable, a model very similar to that describing Lake Erie water levels was obtained. A first order autoregressive model, with a 3 1/2 year lagged MEI as an independent regressor, accounted for 86% of the serial variation associated with Lake Erie outflows. The residuals from this model did not exhibit any significant serial autocorrelation as evidenced by the non-significant Box- Ljung Q statistics in the residual autocorrelation function (see Figure 34). Table 12 (below) summarizes the values of the model parameter estimates. If this table is compared to the table of LEWL-MEI (refer to Table 9), a striking similarity between the two models can be noted, which is to be expected. This provides further verification that the outflow rates are strongly tied to Lake Erie water levels.

Figure 34. Autocorrelation Function
LERO/MEI Residuals From An AR (1) Model
Independent Regressor: MEI - 3 1/2 Year Lag
(Standard errors are white-noise estimates)

Lag	Corr.	S.E.	Q	p
1	-.024	.0735	.10	.7476
2	-.003	.0733	.11	.9487
3	-.020	.0731	.18	.9807
4	+.062	.0729	.91	.9227
5	-.047	.0727	1.32	.9324
6	+.108	.0725	3.53	.7393
7	-.063	.0723	4.29	.7453
8	-.025	.0721	4.42	.8177
9	+.073	.0719	5.45	.7934
10	-.056	.0717	6.07	.8092
11	-.027	.0715	6.21	.8587
12	-.026	.0712	6.35	.8973
13	-.052	.0710	6.89	.9077
14	+.058	.0708	7.57	.9104
15	+.033	.0706	7.80	.9317

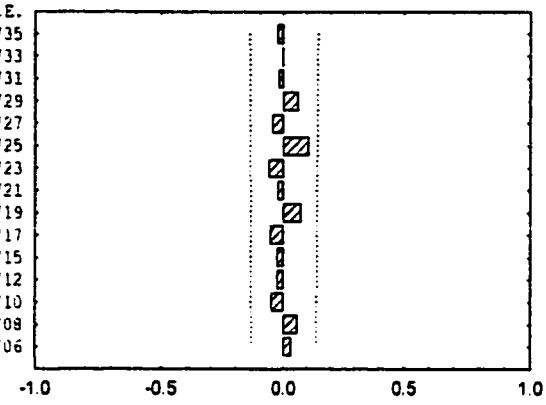

Corr. = Correlation; S.E. = Standard Error
Q = Box-Ljung Q statistic; p = probability value of the Q statistic

TABLE 12. MODEL OF LAKE ERIE OUTFLOWS AND MEI

	B	SEB	T-RATIO	APPROX.	PROB.
AR1	.92561554	.02722086	34.003911	.00000000
MEIQ14	.12125163	.05009588	2.420391	.01649775

(R^2 = .863)

6.8 A Comparison Between MEI and SOI

A multiple regression analysis was run between 1950-1998 semester data of SOI and MEI (where one semester represents a six month time period). Table 13 summarizes the results of the analysis. A very strong relationship exists between the two variables (r = .908), while 82% of the SOI-MEI variations can be accounted for. These results indicate that the Multivariate ENSO Index is a very similar measurement of the El Niño/Southern Oscillation phenomenon as the Southern Oscillation Index. As such, the B.C. temperature/precipitation - SOI analysis presented in chapter 4.2, can be considered relevant to the results found in this research. Also, it appears that if previous research which used the SOI as a measurement of ENSO when comparing the effects of ENSO on atmospheric and/or hydrologic conditions were to have used the Multivariate ENSO Index, similar results would likely have been encountered.

TABLE 13. MULTIPLE REGRESSION RESULTS OF MEI AND SOI
(Statistica '99 Output)

Dependent Variable: MEI (Semester Data)
Multiple R: .908455095 Multiple R-Square: .825290659 Adjusted R-Square: .823470770
Number of cases: 98 F (1, 96) = 453.4841 p < .000000
Standard Error of Estimate: .398953456
Intercept: .001471224 Std. Error: .0404468 t (96) = .03637 p < .971059

7.0 Discussion and Conclusions

7.1 Discussion

The relationship found between Lake Erie water levels and ENSO of 3 1/2 years (lag = 14 quarters) can be accepted under the condition that is recognized that weak impacts of ENSO on Lake Erie water levels are to be expected. It would be inconceivable to expect a strong relationship to exist between the two variables as there are many factors omitted from this research that have the potential of stimulating a change in water balance. Some of these factors include the role of ice cover on the lake, thermal expansion of the lake, temperature patterns, global warming, groundwater effects, consumptive use of water, weed retardation, backwater effects, and anthropogenic changes.

Since there is a significant weak inverse relationship (r = -.153) at lag eight (i.e. two years), it can be claimed that to some extent net basin supplies have responded to El Niño events by falling and La Niña events by rising. It appears as though this lagged inverse relationship is the result of an averaged time lag (relatively speaking) between the effects of ENSO on temperature/air pressure patterns (lag = 3 months) and precipitation (lag = 3 1/4 years) off the west coast of North America. Taking into effect that winters during El Niño conditions tend to experience higher levels of evaporation in those mid-latitude regions controlled by westerly wind systems, it seems logical that at lag 8, an inverse relationship between LENBS and MEI occurs. In all likelihood, El Niño events (with warmer temperatures) are stimulating high levels of evaporation in the Lake Erie basin during the late fall/early winter months. As a result of this, the net basin supply during these months would decrease, as depicted by the inverse cross-correlation at lag 8.

One possible explanation why a stronger relationship does not exist at lag 8, is that during La Niña winters, net basin supplies may not be affected to the same extent as they would be during El Niño winters. La Niña events during winter months tend to be associated with cooler temperatures, that may not have as impacting an effect on the basin supplies. Rather, La Niña

winters may be producing abnormal (enlarged) ice cover on the Great Lakes, which could conceivably lead to a lowering of water levels. Studies are presently ongoing (refer to NOAA website for a complete reference of studies) to see if this is indeed the case.

Lake Erie inflows and outflows (which mimic the temporal behaviour of Lake Erie water levels) have been found to have significant, weak, direct relationships with the Multivariate ENSO Index, after a 3 1/2 year lagged time period (LSCO: .155; LERO: .161). As a result, it can be claimed that to a certain degree the primary flows of water into and out of Lake Erie have responded to El Nino events by increasing in volume and velocity and to La Nina events by decreasing in volume and velocity. Weak impacts of ENSO on the flows of water entering and leaving the lake should be expected. The omitted factors (from this research) that have the potential of stimulating a change in water levels, also apply here. For example, weed growth alone in the Niagara River from June to October reduces Lake Erie outflows by about 50 to 225 m^3/s (Lee et al., 1998).

An eighteen month (i.e. 6 quarters) time lag has been found to exist between the effects of ENSO on Lake Erie net basin supply and Lake Erie water levels and flows. This can be explained by the following logic. It takes 3 1/4 years for B.C. rainfall to be significantly affected by an El Niño or La Niña event. Factoring in a modest lag time for the rainwaters to hit the Lake Erie basin, a 3 1/2 year lag time for the water levels and flows to change (from precipitation) is certainly realistic. If this is the case, then it seems apparent that evaporation rates may be near or equal to precipitation levels at lag 14 in the system. An equal balance of precipitation and evaporation in the system would effectively eliminate any chance of the Multivariate ENSO Index being correlated with Lake Erie net basin supply at lag 14. Therefore, it is recommended that in future research the components of net basin supply be tested on an individual basis, rather than as a computed sum. This would help pinpoint the time lag(s) it takes for ENSO events to have influencing effects on specific atmospheric and hydrologic variables within the Great Lakes region.

7.2 Conclusions

This research was able to determine the long-term (psuedo -) cyclic fluctuations of not only the Lake Erie water balance components under study, but also the El Niño/Southern Oscillation phenomenon (measured using the Multivariate ENSO Index). Each time series examined clearly shows the presence of stochastic processes in effect. The time-ordered findings here complement the findings of others such as Guetter et al. (1995), LaValle et al. (1999), and Wang et al. (1999).

The temporal behaviour findings of the Lake Erie hydrologic variables have been cross-correlated and regressed with the Multivariate ENSO Index to assess the possibility of existing relationships with ENSO events. A two year lagged weak inverse relationship was discovered to exist between Lake Erie net basin supply data and MEI. A three and a half year lagged direct relationship existed between Lake Erie inflows, water levels, and outflows and the Multivariate ENSO Index. These findings can be considered as an initial step towards understanding the water balance changes within Lake Erie. Further studies are required on the effects of ice cover, anthropogenic changes, and backwater, before any conclusive inferences about the relationships between Lake Erie water level dynamics and ENSO can be made.

Hydrologists and shoreline engineers continue to model the nature of water level dynamics in an attempt to provide the most effective shoreline protection strategies possible. Short-term changes in water levels can prompt quick decisions on implementation strategies such as dredging, infilling, or employing the use of beach structures such as groynes, jetties, or concrete tetrapods. Ill-advised implementations can lead to severe adverse effects over the long-term (Lee et al., 1998; Quinn, 1999), and thus the importance of knowing the contributing factors to water level change becomes critical. If the factors and their associated temporal cycles (if applicable) are known, implementation strategies and modelling future scenarios decrease in difficulty. This research cautiously relates the ENSO phenomenon with fluctuating Lake Erie water levels. It is now left up to future researchers to verify and expand upon the statistical results found here. By

doing so, a more effective means of coping with the dynamics of water level change in the Great Lakes may become feasible.

7.3 Limitations Associated with the Multivariate ENSO Index

Because the MEI is a relatively new measure of the state of ENSO, little research has been completed using the MEI as an independent regressor variable. As such, this study's findings represent a stepping stone to build from, and should not be considered as definitive. The El Niño/Southern Oscillation phenomenon can be considered to have marginal effects on the water levels and flows of Lake Erie, but these effects should be approached with caution. More research is required on the viability of the MEI, in both a regional and global context, before any definitive conclusions can be made.

Further verification on the multiple regression analysis results between SOI and MEI is required. It needs to be determined if multiple regression techniques can accurately describe the relationship between the two ENSO measurements. Future studies of the relationship between Great Lakes water levels and the ENSO phenomenon may be best served to incorporate both the Southern Oscillation Index and MEI, to determine any differences the two indices may have. This would help validate (or in-validate) the findings of both LaValle et al. (1999) which used the SOI to measure ENSO, and the research presented here.

References

Ahrens, C.D. 1993. *Essentials of meteorology: An invitation to the Atmosphere*. St. Paul, MN: West Publishing Company.

Battisti, D.S., and Hirst, A.C. 1989. Interannual variability in the tropical atmosphere/ocean system: Influence of the basic state and ocean geometry. *Journal of the Atmospheric Sciences*, 46: 1687-1712.

Bennett, R.J. 1979. *Spatial time series*. London: Pion Limited.

Box G.E.P., and Jenkins, G.M. 1976. *Time series analysis: forecasting and control*. Revised edition. San Francisco, CA: Holden-Day.

Bjerknes, J. 1969. Atmospheric teleconnections from the equatorial Pacific. *Monthly Weather Review.*, 97: 163-172.

Bruce, J.P. 1984. 'Great Lakes levels and flows: past and future', *Journal of Great Lakes Research*, 10 (1): 126-134.

Brunk, I.W. 1964. Hydrology of Lakes Erie and Ontario. In *Proc. 7th Conf. On Great Lakes Res.*, pp.205-216. Inernat. Assoc. Great Lakes Res.

Cane, M.A., and Zebiak, S.E. 1985. A theory for El Nino and the Southern Oscillation. *Science*, 228: 1084-1087.

Cane, M.A., Zebiak, S.E., and Dolan, S.C. 1986. Experimental forecasts of El Nino. *Nature*, 321: 827-832.

Chatfield, C. 1975. *The analysis of time series: An introduction*. London and New York: Chapman and Hall.

Derecki, J.A. 1976. Multiple estimates of Lake Erie evaporation. *J. Great Lakes Res.* 1: 124-149.

Diaz, H.F., and Kiladis, G.N. 1992. Atmospheric teleconnections associated with the extreme phase of the Southern Oscillation. In *El Nino. Historical and paleoclimatic aspects of the Southern Oscillation*, eds. H.F. Diaz and V. Markgraf, pp. 7-28. Cambridge, UK: Cambridge University Press.

Environment Canada and U.S. Environmental Protection Agency. 1995. *Great Lakes Atlas*.

Guetter, A., and Georgakakos, K. 1996. Are the El Nino and La Nina predictors of the Iowa River seasonal flow? *Journal of Applied Meteorology*, 35: 690-705.

International Great Lakes Levels Board (IGLLB). 1973. *Regulation of Great Lakes water levels*. Report to the Intenational Joint Commission, Washington, D.C. and Ottawa, Ontario.

Jin, F.-F. 1997. An equatorial ocean recharge paradigm for ENSO (Parts I and II). *Journal of Atmospheric Sciences*, 54: 811-847.

Jin, F.-F. 1998. A simple model for the Pacific cold tongue and ENSO. *Journal of the Atmospheric Sciences*, 55: 2458-2469.

Jin, F.-F., and Neelin, J.D. 1993. Modes of interannual tropical ocean-atmosphere interaction - A unified view. Part I: Numerical results. *Journal of the Atmospheric Sciences*, 50: 3477-3502.

Jones, D.M.A., and Meredith, D.D. 1972. Great Lakes hydrology by months, 1946-65. In *Proc. 15th Conf. on Great Lakes Res.*, pp. 477-506. Internat. Assoc. Great Lakes Res.

Kane, R.P. 1997. Relationship of El Nino-Southern Oscillation and Pacific sea surface temperature with rainfall in various regions of the globe. *Monthly Weather Review*, 125: 1792-1800.

Kiladis, G.N., and Diaz, H.F. 1989. Global climate anomalies associated with extremes in the Southern Oscillation. *Journal of Climate*, 2: 1069-1090.

Kite, G.W. 1992. Simulation of Lake Erie mean monthly water levels. *Journal of Great Lakes Research*, 18(3): 481-488.

LaValle, P.D., and Lakhan, V.C. 1997. A spatial-temporal analysis of the development of a log-spiral shaped embayment. *Earth Surface Processes and Landforms*, 22: 657-667.

LaValle, P.D., Lakhan, V.C., and Trenhaile, A.S. 1999. Short-term fluctuations of Lake Erie water levels and the El Niño/Southern Oscillation. *The Great Lakes Geographer.*

LaValle, P.D. 2000. Personal communication - based on research in an upcoming journal article.

Lee, D., Quinn, F., Clites, A. 1998. Effect of the Niagara River Chippawa Grass Island Pool on water levels of Lakes Erie, St. Clair, and Michigan-Huron. *Journal of Great Lakes Research*, 24 (4): 936-948.

Meadows, G.A., Meadows, L.A., Wood, W.L., Hubertz, J.M., and Perlin, M. 1997. The relationship between Great Lakes water levels, wave energies, and shoreline damage. *Bulletin of the American Meteorological Society*, 4: 675-683.

NOAA website (http://coastwatch.glerl.noaa.gov/statistic/physical.html). 1999. *Physical characteristics of the Great Lakes.*

NOAA website (http://www.cdc.noaa.gov/~kew/MEI/). *Multivariate ENSO Index (MEI).*

Philander, S.G. 1990. *El Nino, La Nina, and the Southern Oscillation*. San Diego, CA: Academic Press, Inc.

Quinn, F.H. 1978. Hydrologic response model of the North American Great Lakes. *Journal of Hydrology*, 37: 295-307.

Quinn, F., and Guerra, B. 1986. Current perspectives on the Lake Erie water balance. *Journal of Great Lakes Research*, 12: 109-116.

Quinn, F., and Neal, V.T. 1992. The historical record of El Nino events. In *Climate since A.D. 1500*, eds. R.S. Bradley and P.D. Jones, pp. 623- 648. London and New York: Routledge.

Quinn, F.H. 1999. Anthropogenic changes to Great Lakes water levels. *Great Lakes Update*, No. 136.

Ropelewski, C.F., and Halpert, M.S. 1986. North American precipitation and temperature patterns associated with the El Nino/Southern Oscillation (ENSO). *Monthly Weather Review*, 114: 2353-2362.

Ropelewski, C.F., and Halpert, M.S. 1987. Global and regional scale precipitation patterns associated with the El Niño/Southern Oscillation. *Monthly Weather Review*, 115: 1606-1626.

Ropelewski, C.F., and Halpert, M.S. 1989. Precipitation patterns associated with the high index phase of the Southern Oscillation. *Journal of Climate*, 2: 268-289.

Salas, J.D., Delleur, J.W., Yevjevich, V., and Lane, W.L. 1980. *Applied modeling of hydrologic time Series.* Colorado: Water Resources Publications.

Sanderson, M.E. 1966. The 1958-63 water balance of the Lake Erie basin. *In Proc. Ninth Conf. on Great Lakes Res.*, pp. 274-282. Great Lakes Res. Div., Univ. Mich., Ann Arbor, Michigan.

Sanderson, M. 1993. Climate change and water in the Great Lakes basin. *Canadian Water Resources Journal*, 4: 417-424.

Schopf, P.S., and Suarez, M.J. 1988. Vacillations in a coupled ocean-atmosphere model. *Journal of Atmospheric Sciences*, 45: 549-566.

Shabbar, A., and Khandekar, M. 1996. The impact of El Niño-Southern Oscillation on the temperature field over Canada. *Atmosphere-Ocean*, 34 (2): 401-416.

Shabbar, A., Bonsal, B., and Khandekar, M. 1997. Canadian precipitation patterns associated with the Southern Oscillation. *Journal of Climate*, 10(12): 3016-3027.

Stone, R.C., Hammer, G.L., and Marcussen, T. 1996. Prediction of global rainfall probabilities phases of the Southern Oscillation Index. *Nature*, 384: 252-255.

Thompson, R.D., Mannion, A.M., Mitchell, C.W., Parry, M., and Townshend, J.R.G. 1986. *Processes in physical geography.* New York, NY: Longman.

Vandaele, W. 1983. *Applied time series and Box-Jenkins models.* Academic Press, Inc.

Wang, B., Barcilon, A., and Fang, Z. 1999. Stochastic dynamics of El Nino-Southern Oscillation. *Journal of the Atmospheric Sciences*, 56: 5-23.

Waylen, P.R., Caviedes, C.N., and Juricic, C. 1993. El Nino-Southern Oscillation and the surface hydrology of Chile: A window on the future? *Canadian Water Resources Journal*, 4: 425-441.

Wolter, K. 1987. The Southern Oscillation in surface circulation and climate over the tropical Atlantic, Eastern Pacific, and Indian Oceans as captured by cluster analysis. *Journal of Climate and Applied Meteorology*, 26: 540-558.

Wolter, K., and Timlin, M.S. 1993. Monitoring ENSO in COADS with a seasonally adjusted principal Component index. *Proc. of the 17th Climate Diagnostics Workshop*, Norman, OK, NOAA/N MC/CAC, NSSL, Oklahoma Clim. Survey, CIMMS and the School of Meteor., Univ. of Oklahoma, 52-57.

[illegible]. *Lake Erie.*

[illegible]. *Factors affecting GreatLakes-St. Lawrence system flows.*

Wyrtki, K. 1985. Water displacements in the Pacific and the genesis of El Nino cycles. *Journal of Geophysical Research*, 91: 7129-7132.

Appendix: General Circulation of the Atmosphere

The actual flow of air is complex; to this day not everything is known about it. What is known is that the underlying cause of the general circulation (defined in Ahrens (1993) as the average air flow around the world; actual winds may vary considerably from this average at any place or time) is the unequal heating of the earth's surface. The three-cell model will be outlined to help eliminate some of the complexities of the general circulation. It must be noted that outline is provided to give a general knowledge of the circulation processes of the earth, and in no way does it attempt to explain atmospheric interactions/processes on a micro-scale level.

The Three-Cell Model

In each hemisphere, there are three rotating convection cells that have the task of energy redistribution. Tropical regions receive an excess of heat and the poles face a deficit. By examining what happens to air above the equator, a modest explanation of the three-cell model (outlined in Ahrens, 1993) can be given.

a) ***The Hadley Cell***

Over equatorial waters, warm air exists along with weak horizontal pressure gradients and light winds. Known as the doldrums region, rising warm air reaches the tropopause, which acts like a barrier, causing the air to move laterally towards the poles. The Coriolis force (an apparent force that is due to the rotation of the earth; magnitude of force can be determined by the equation (in Thompson et al., 1986): $f = 2\omega V \sin\phi$; where ω is the angular velocity of spin about the vertical, V is the horizontal speed of the air, and ϕ is the latitude) deflects this poleward flow toward the right in the northern hemisphere and to the left in the southern hemisphere, providing westerly winds aloft in both hemispheres.

At latitudes near 30°, the convergence of air aloft produces produces belts of high pressure called subtropical highs (anticyclones). From these latitudes, some of the surface air moves back toward the equator (the air blows from the northeast in the northern hemisphere and the southeast in the southern hemisphere) due to a deflection process by the Coriolis force. This air

is classified as the trade winds. Near the equator, the northeast trades converge with the southeast trades along a boundary called the intertropical convergence zone (ITCZ). This zone of surface convergence allows air to rise and continue its cellular journey (completing the Hadley cell).

b) ***The Middle Cell***

Not all of the surface air moves equatorward at latitudes near 30°. Some of the air moves towards the poles and deflects toward the east, resulting in a westerly air flow known as the westerlies (or prevailing westerlies). This flow is not constant, as from time to time migrating areas of high and low pressure break up the surface flow pattern.

As mild air travels poleward, it encounters cold air moving down from the poles. These two air masses of contrasting temperature do not readily mix. The air masses are separated by a boundary known as the polar front, a zone of low pressure (the subpolar low) where surface air converges and rises and storms develop. Some of the rising air returns at high levels to the horse latitudes where it sinks back in the vicinity of the subtropical high. The middle cell of the three-cell model is completed when surface air from the horse latitudes flows poleward toward the polar front.

c) ***The Polar Cell***

Behind the polar front, the cold air from the poles is deflected by the Coriolis force. This results in a general flow of northeasterly air. Subsequently, this region is termed the polar easterlies. During the winter season, the polar front can move into middle and subtropical latitudes, producing a cold polar outbreak. Along the front, a portion of the rising air moves poleward, and the Coriolis force deflects the air into a westerly wind at high levels. Air aloft circulates toward the poles, sinks in a slow manner to the surface, and flows back toward the polar front, completing the polar cell.

Vita Auctoris

Chris Johnston was born in 1975 in Sarnia, Ontario. He graduated with an Honours Degree in Geography from the University of Windsor in 1998.

UNIVERSITY OF
WINDSOR

To: **Senate**
From: **John Corlett, Chair**
Senate Steering Committee
Re: **Senate Committees**

Date: **May 25, 2000.**

Following is the recommended slate of officers as recommended by the Senate Steering Committee.

Senate Steering Committee

Administrative Dean of Student and Academic Services/Registrar (Chair)
John Corlett

President
Ross Paul

Vice-President, Academic
Neil Gold

The College of Graduate Studies and Research

Kate McCrone	1999-2001
Barbara Thomas	2000-2001

The College of Engineering and Science

Brian Atkinson	2000-2001
Nihar Biswas	2000-2001

The College of Business Administration, Education and Law

Anne Forrest	2000-2001
Brian Mazer	2000-2001

The College of Arts and Human Sciences

David Palmer	2000-2001
Susan Wendt-Hildebrandt	1999-2001

Librarian

Johanna Foster	1999-2001

Student Representation

TBA (SGPS)	2000-2001
Ed King (OPUS)	2000-2001
TBA (UWSA)	2000-2001
TBA	2000-2001

Program Development Committee

Vice-President, Academic (Chair)

Neil Gold

The College of Graduate Studies and Research

Sheila Cameron	2000-2001
Bulent Mutus	2000-2001
Jim Weese	2000-2001

The College of Engineering and Science

Rick Caron	2000-2001
* Alan Cook	2000-2001
Graham Reader	2000-2001

The College of Business Administration, Education and Law

Linda MacKay	2000-2001
Alfie Morgan	2000-2001
Jeff Berryman	2000-2001

The College of Arts and Human Sciences

Kate McCrone	2000-2001
Diana Mady Kelly	2000-2001
Veronica Mogyorody	2000-2001

Librarian

Gwenn Ebbett	1999-2001

Student Representation

TBA (SGPS)	2000-2001
Marty Lowman(OPUS)TBA	2000-2001
TBA(UWSA)	2000-2001
TBA	2000-2001

CLERK OF THE SENATE
401 SUNSET • WINDSOR ONTARIO • CANADA N9B 3P4 • 519/253-4232

Academic Policy Committee

Associate Vice-President, Academic, (Chair)
Mike Salter

Vice-President, Administration and Finance

Eric Harbottle

The College of Graduate Studies and Research

Ann Snowdon	2000-2001
David Symons	2000-2001
Dietmar Lage	1999-2001

The College of Engineering and Science

Alden Warner	2000-2001
Andrzej Sobiesiak	1999-2001
Harold Atkinson	2000-2001

The College of Arts and Human Sciences

Mary Gold	2000-2001
Tony Blair	1999-2001
Ihor Stebelsky	1999-2001

The College of Business Administration, Education and Law

*	2000-2001
Donna Green	2000-2001
Noel Hurley	2000-2001

Librarian

Cynthia Archer	1999-2001

Student Representation

TBA (SGPS)	2000-2001
Ed King (OPUS)	2000-2001
TBA (UWSA)	2000-2001
TBA	2000-2001

Student Committee

Administrative Dean of Student and Academic Services/Registrar (Chair)

John Corlett

The College of Graduate Studies and Research

*	2000-2001
Frank Lemire	2000-2001
Lesley Lovett-Doust	2000-2001

The College of Engineering and Science

Michael Dufresne	2000-2001
Ahmet Alpas	1999-2001
Dale Rajacich	2000-2001

The College of Arts and Human Sciences

Heather MacIvor	2000-2001
Susan Gold Smith	2000-2001
Norman King	2000-2001

The College of Business Administration, Education and Law

Bill Wellington	1999-2001
Norm Diffey	2000-2001
Larrry Glassford	2000-2001

Librarian

Joan Dalton	1999-2001

Student Representation

TBA (SGPS)	2000-2001
Mary Lou Gelissen (OPUS)	2000-2001
TBA(UWSA)	2000-2001
TBA	2000-2001